RG-K DVCS Analysis:
Beam Spin Asymmetry Measurements at 6.5 GeV and 7.5 GeV

Joshua Artem Tan

23 June 2025

Contents

Introduction

Towards GPDs to GFFs

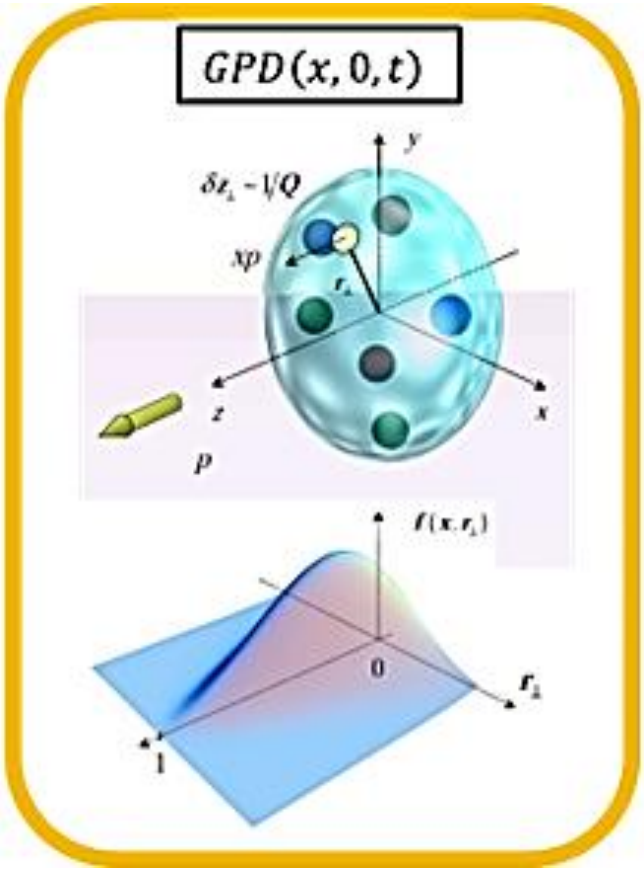

H GPD to $d_1(t)$ GFF

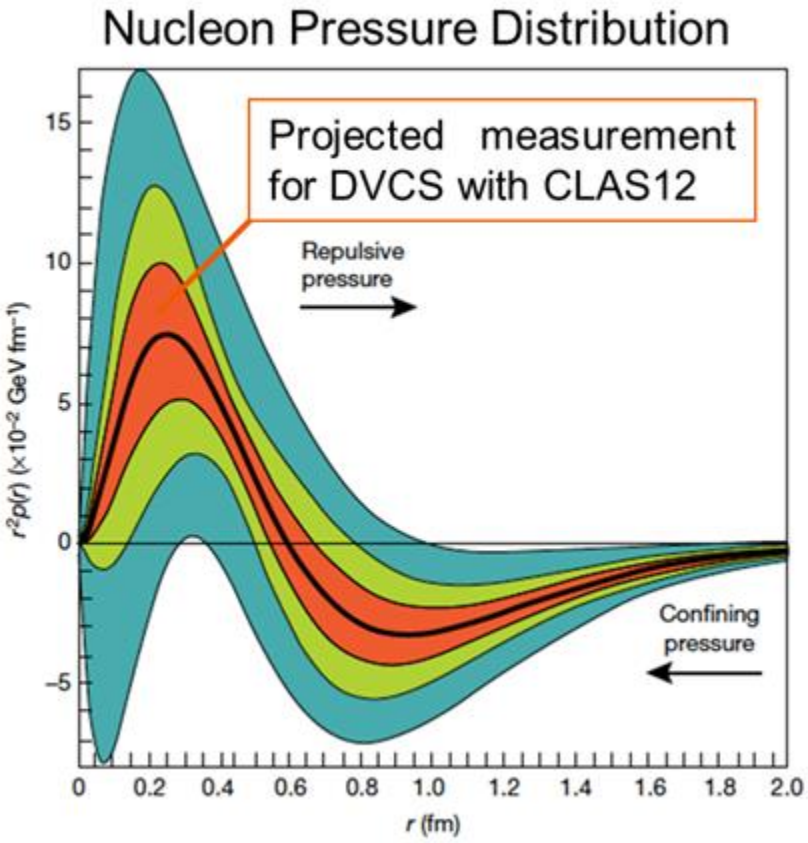

Deeply Virtual Compton Scattering (DVCS) provides cleanest access to GPDs. Beam Spin Asymmetry is particularly sensitive to H GPD from which the GFF $d_1(t)$ can be extracted.

$ep \rightarrow e'p'\gamma$ Reaction

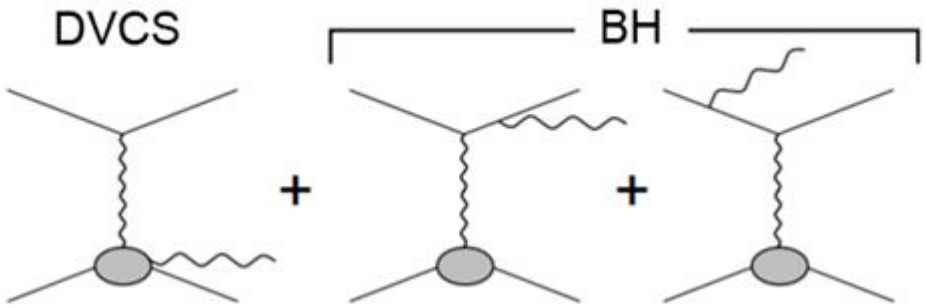

$$|\mathcal{T}|^2 = |\mathcal{T}_{\mathrm{DVCS}}|^2 + |\mathcal{T}_{\mathrm{BH}}|^2 + \mathcal{I}$$

$$A_{\mathrm{LU}}(\phi) = \frac{d\sigma^{\uparrow}(\phi) - d\sigma^{\downarrow}(\phi)}{d\sigma^{\uparrow}(\phi) + d\sigma^{\downarrow}(\phi)} \Rightarrow A_{\mathrm{LU}}(\phi) \approx \frac{x_B(1+\epsilon^2)^2}{y} \frac{s^{\mathcal{I}}_{1,\mathrm{unp}} \sin(\phi)}{c^{\mathrm{BH}}_{0,\mathrm{unp}} + c^{\mathrm{BH}}_{1,\mathrm{unp}} \cos(\phi)}$$

$$\alpha \equiv \frac{x_B(1+\epsilon^2)^2 s^{\mathcal{I}}_{1,\mathrm{unp}}}{y c^{\mathrm{BH}}_{0,\mathrm{unp}}}, \beta \equiv \frac{c^{\mathrm{BH}}_{1,\mathrm{unp}}}{y c^{\mathrm{BH}}_{0,\mathrm{unp}}} \Rightarrow A_{\mathrm{LU}}(\phi) \approx \frac{\alpha \sin(\phi)}{1 + \beta \cos(\phi)}$$

$$\alpha \propto \Im\mathfrak{m}\left[F_1\mathcal{H} + \frac{x_B}{2 - x_B}(F_1 + F_2)\widetilde{\mathcal{H}} - \frac{\Delta^2}{4M^2}F_2\mathcal{E}\right]$$

BSA is an observable measured from the DVCS-BH interference term of $ep \rightarrow e'p'\gamma$ reaction's scattering amplitude.

Beam Spin Asymmetry

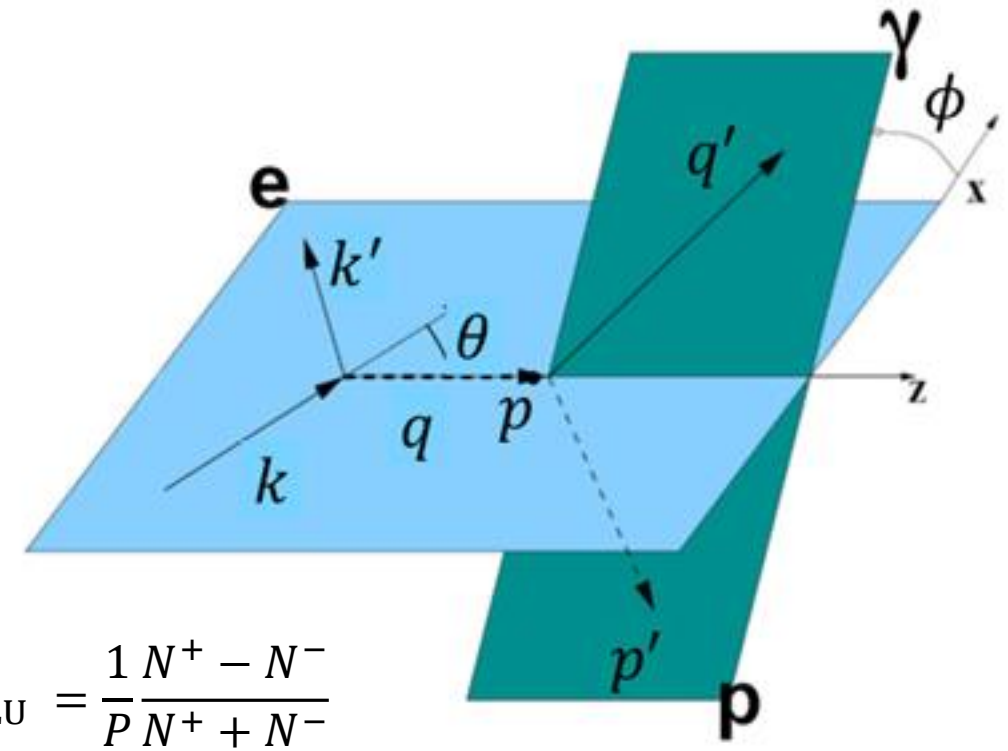

$$A_{\mathrm{LU}} = \frac{1}{P}\frac{N^{+} - N^{-}}{N^{+} + N^{-}}$$

BSA shows the relative cross-section difference of positive and negative beam helicity events as function of the separation angle between the lepton and the reaction planes.

Experiment

CLAS12 Configuration

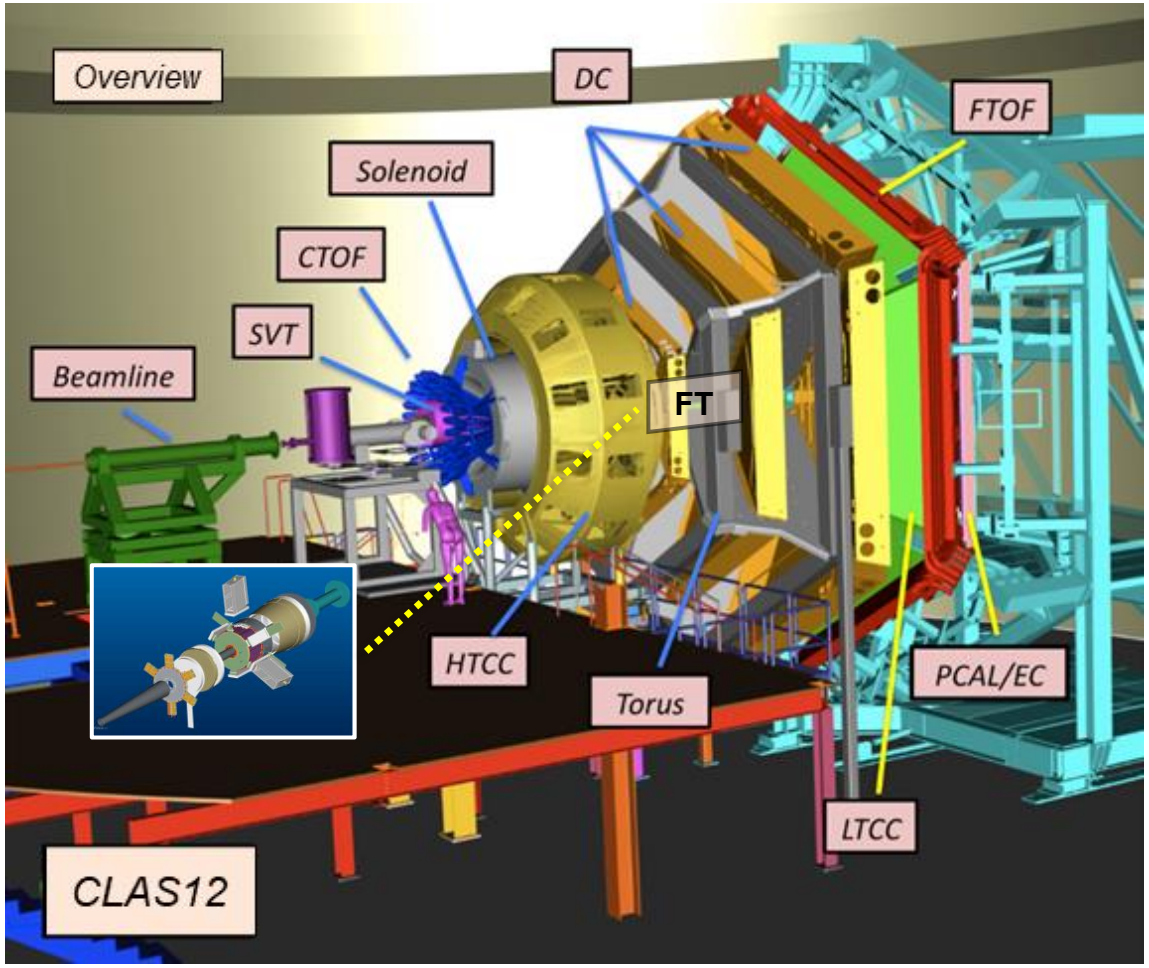

6.5 GeV experiment was performed with the Forward Tager (FT) off, and 7.5 GeV experiment was run with FT on.

Run Conditions

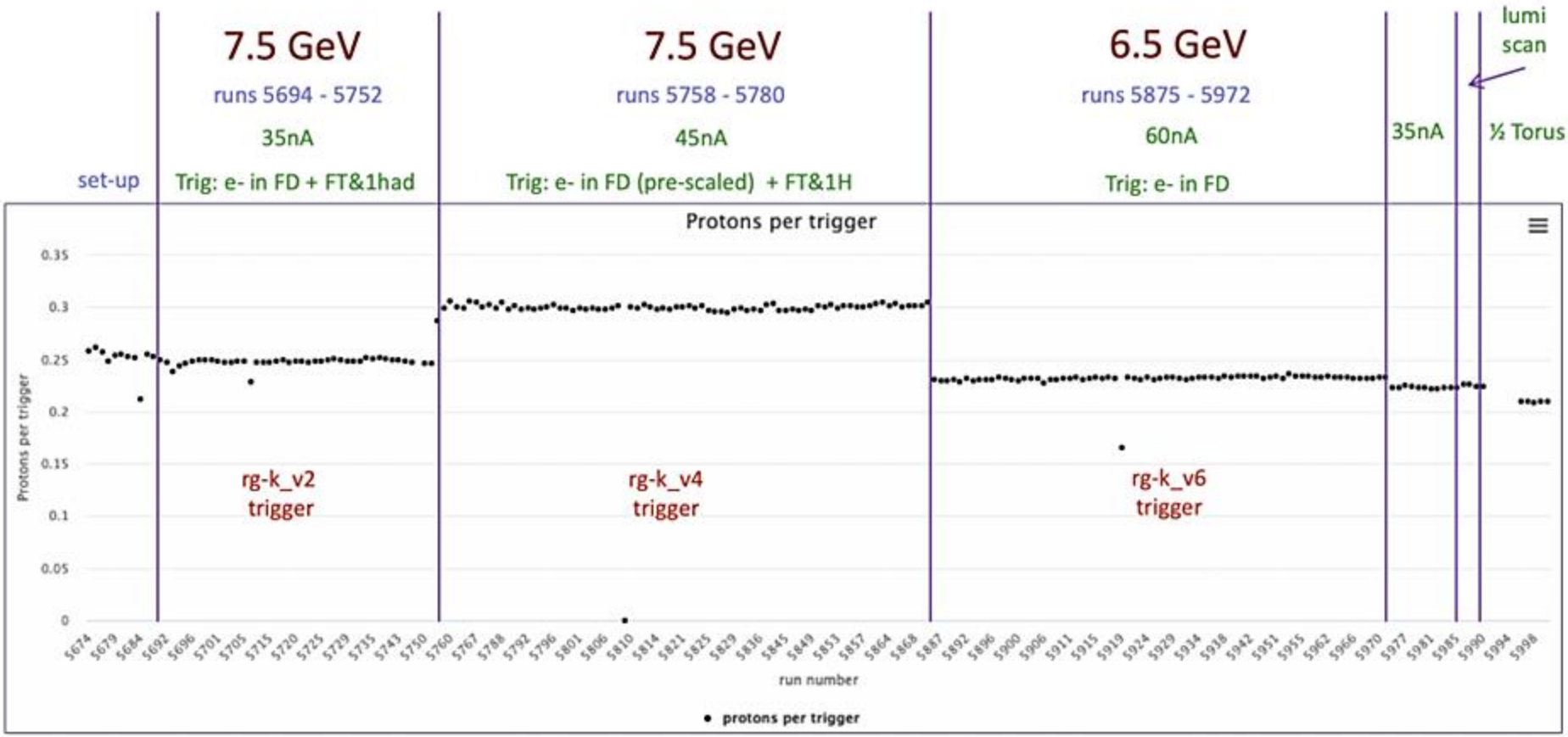

6.5 GeV beam was measured with 85.17±1.49% polarization and 7.5 GeV beam had 86.17±1.49% polarization.

Fiducial Cuts

ECal Fiducial Cuts

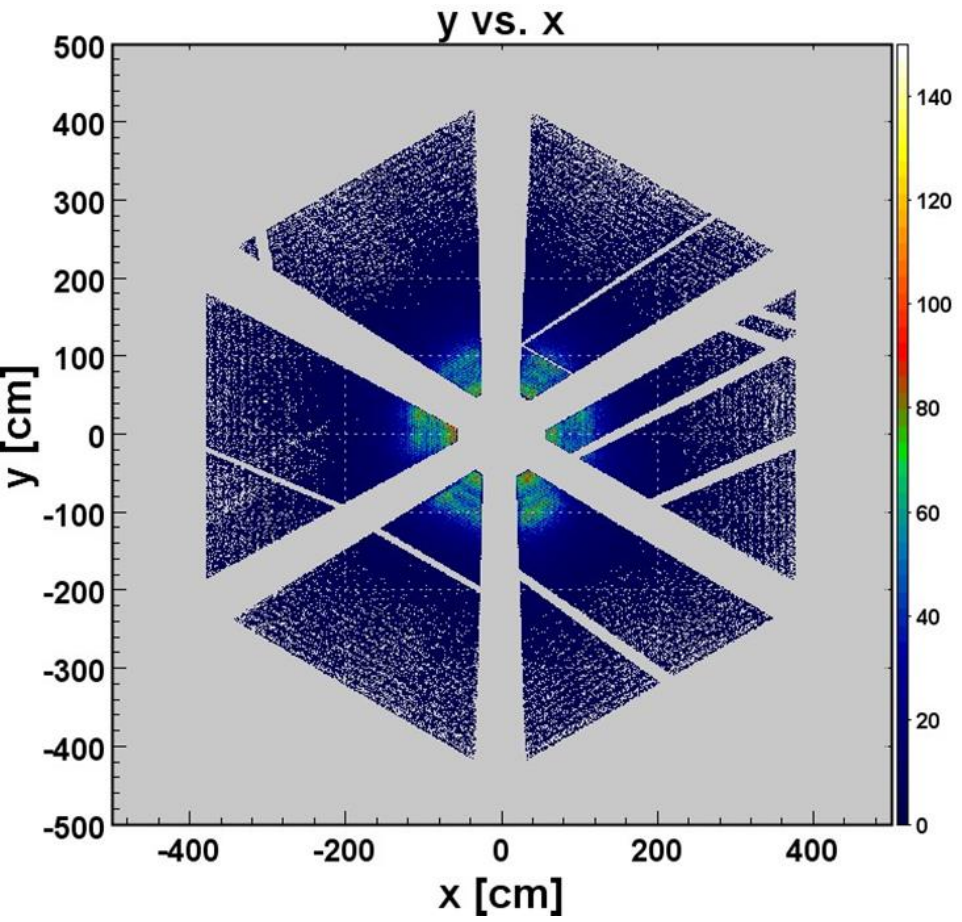

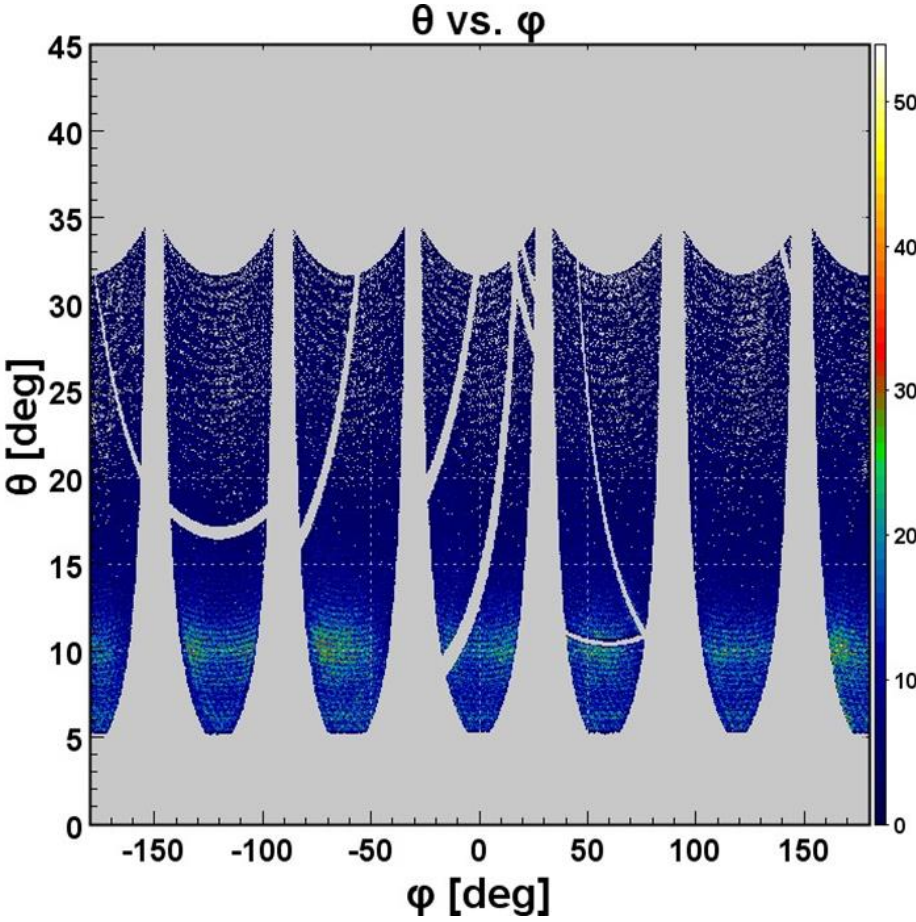

ECal fiducial was defined by cutting off the “rough” edges and regions corresponding to faulty channels on the hit map.

FTCal Fiducial Cuts

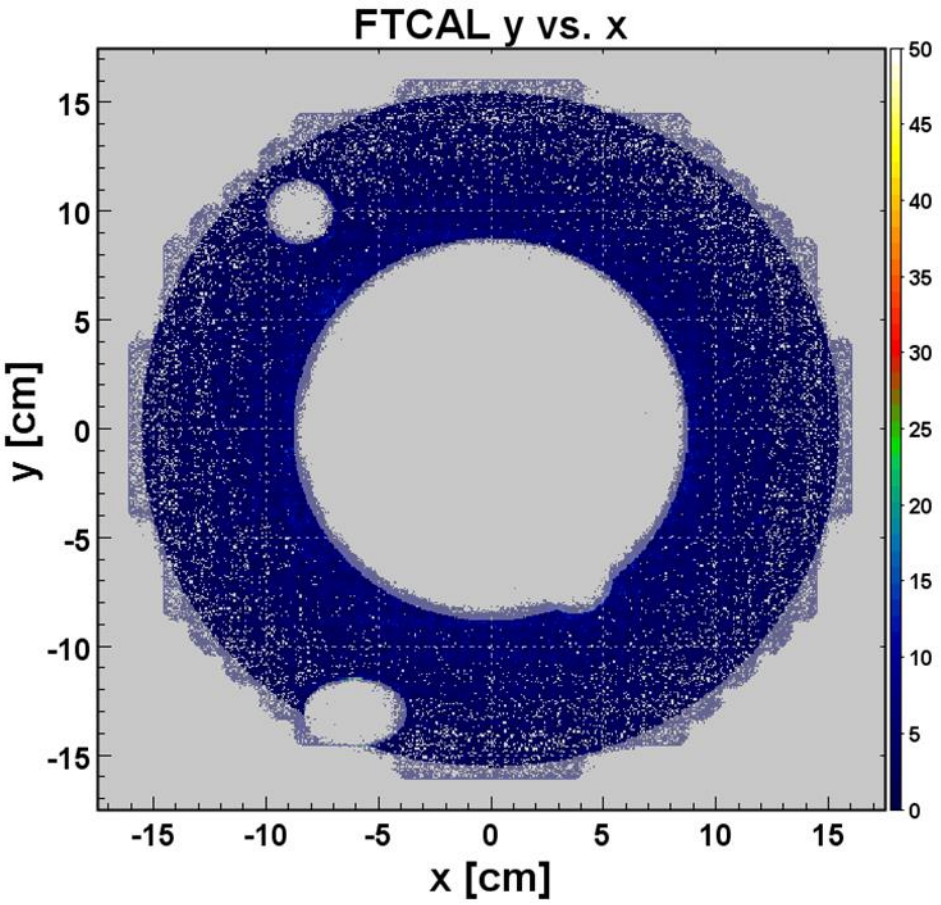

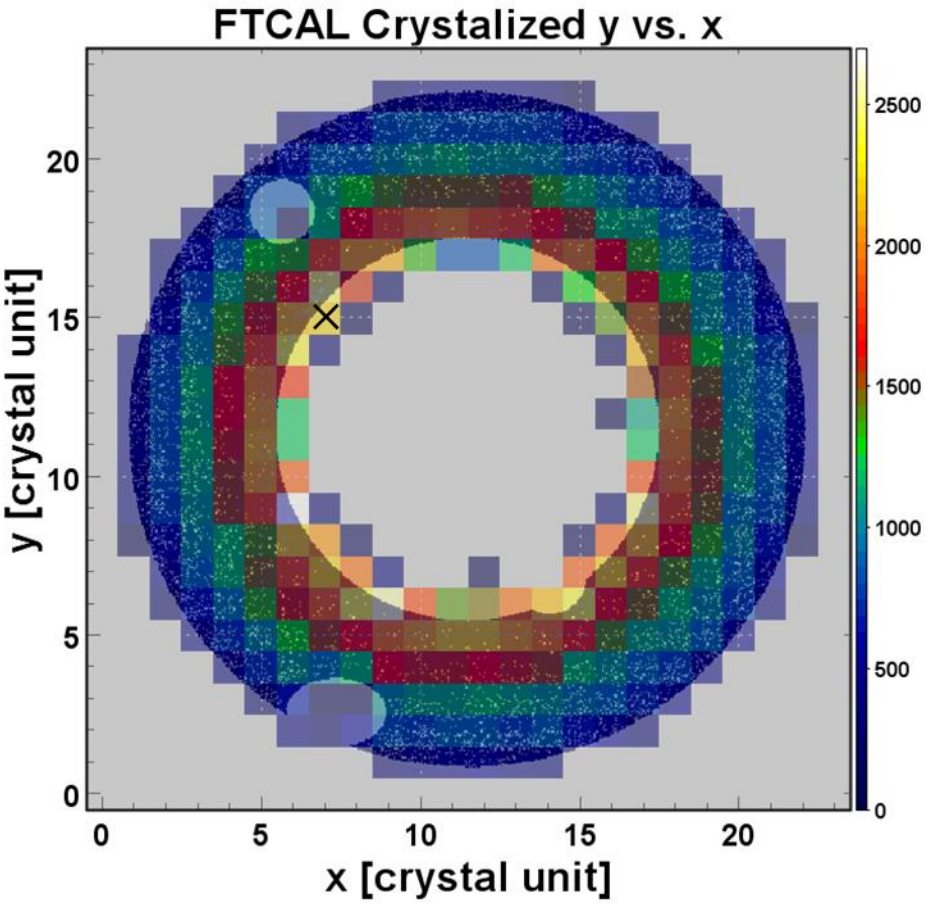

FTCal fiducial was trimmed to exclude both “rough” edges and pixels corresponding to faulty channels on the hit map.

Kinematic Corrections

Electron Momentum Correction

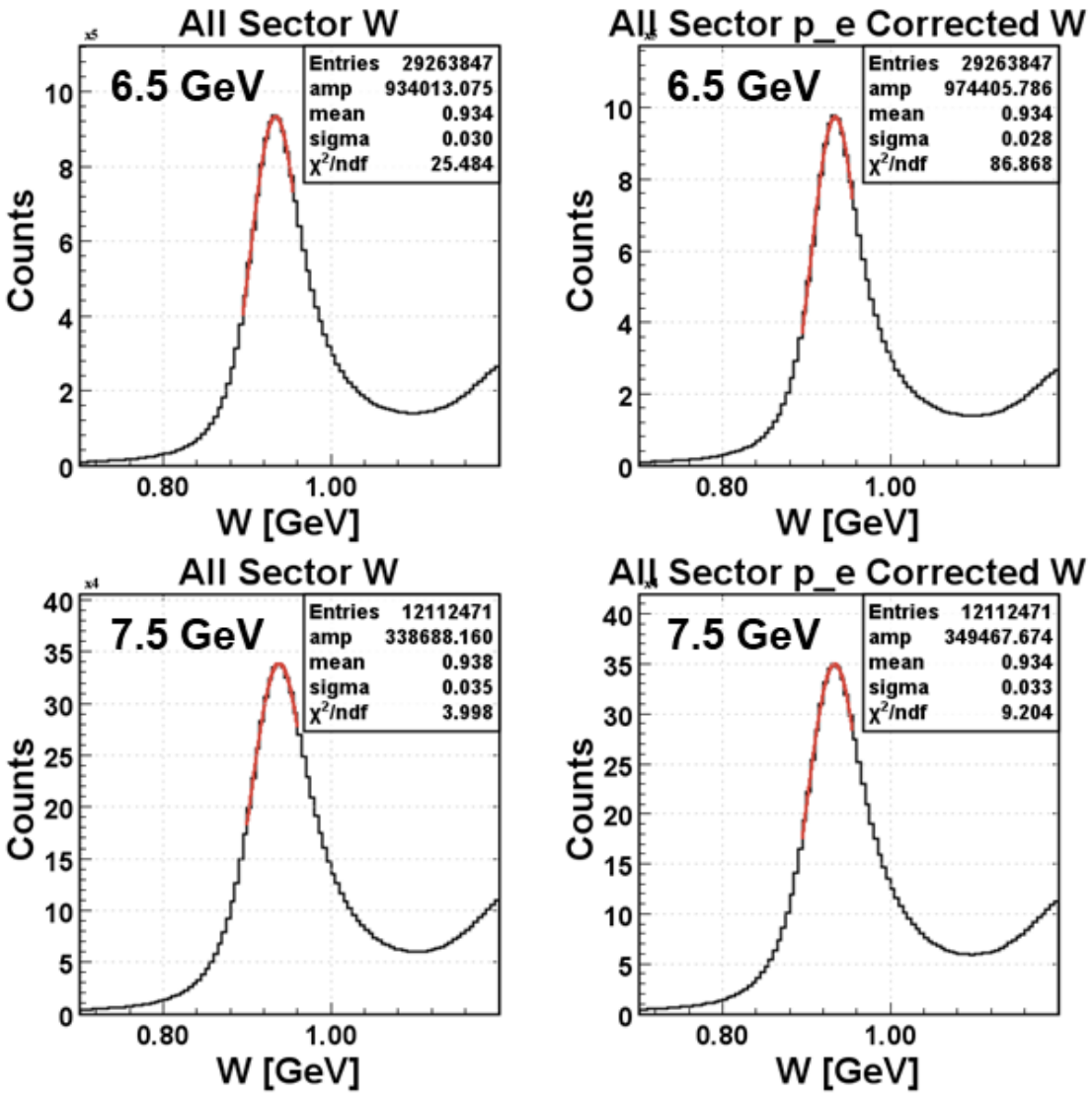

These elastic-channel-based corrections were implemented by parameterizing δW in lab-frame θ and φ of the scattered e.

Proton Momentum Correction

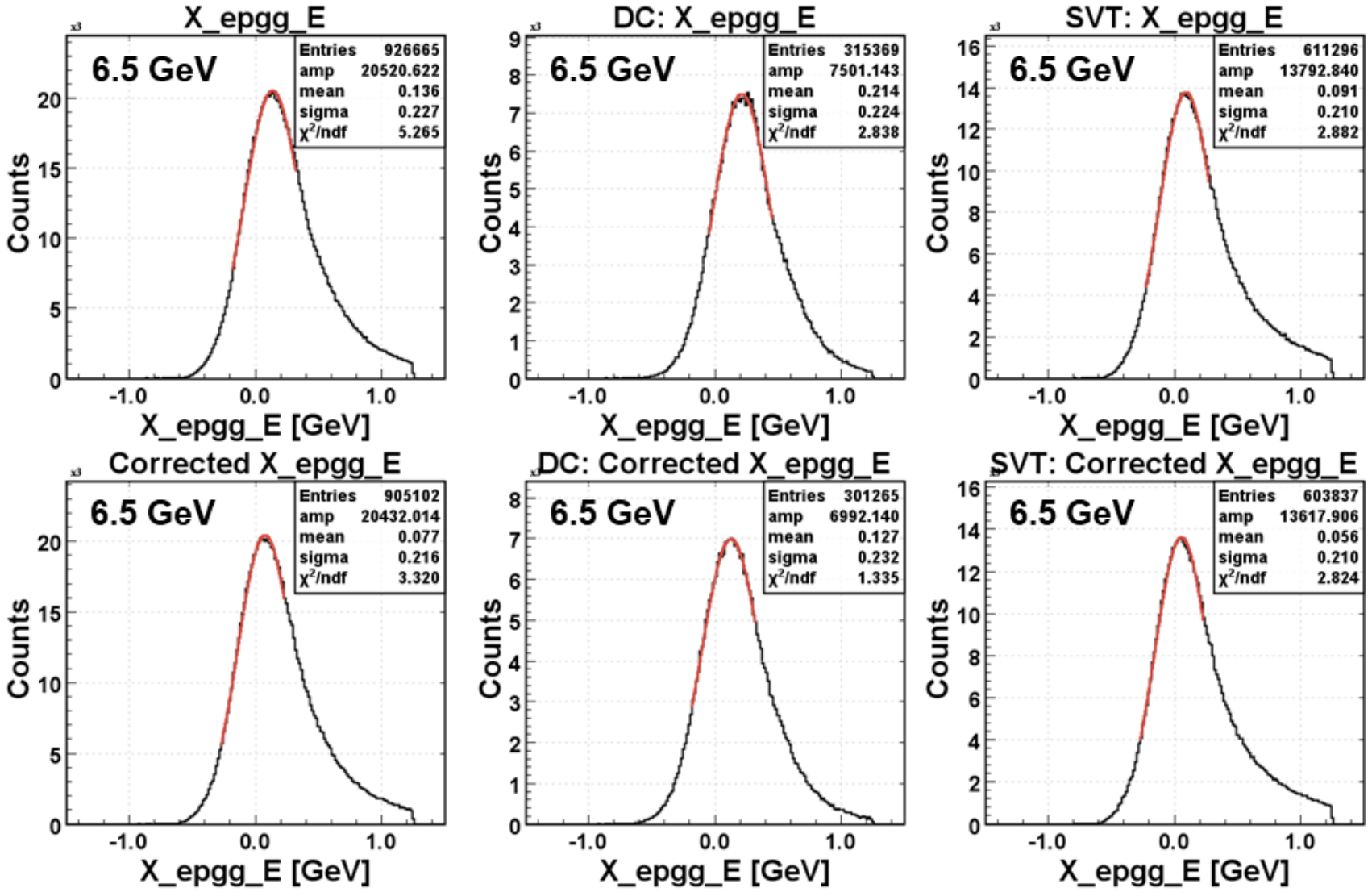

These corrections were implemented by parameterizing δE_X in lab-frame θ and φ of p' from exclusive $ep \rightarrow e'p'(\gamma\gamma)_{\pi^0}$.

Event Selection

6.5 GeV Acceptance

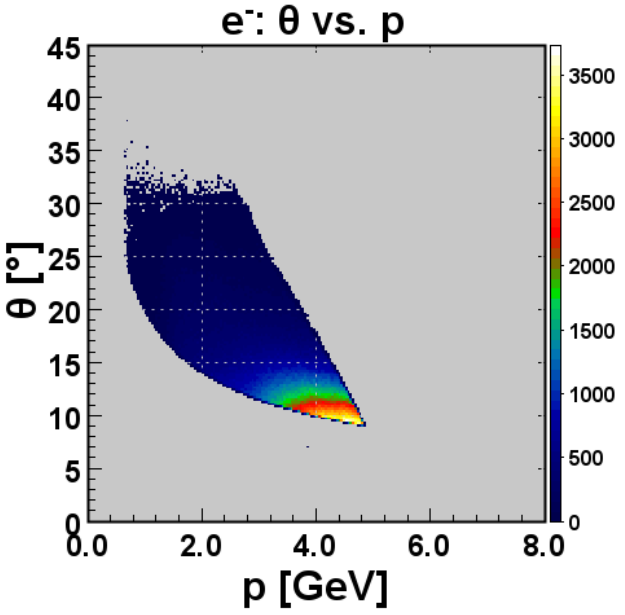

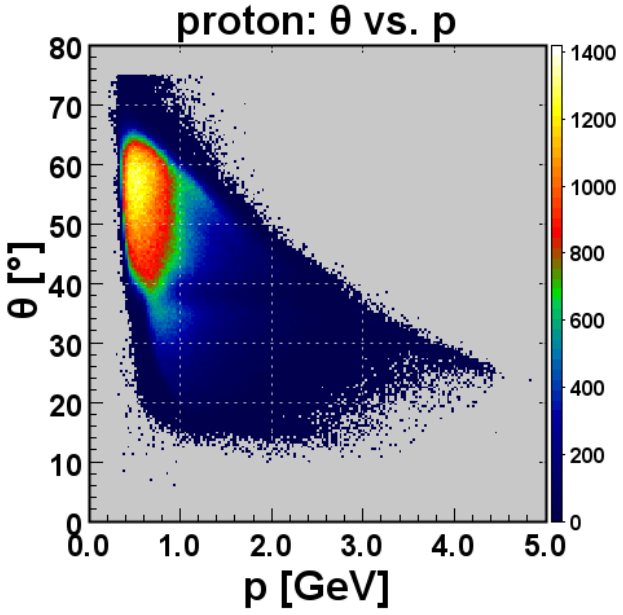

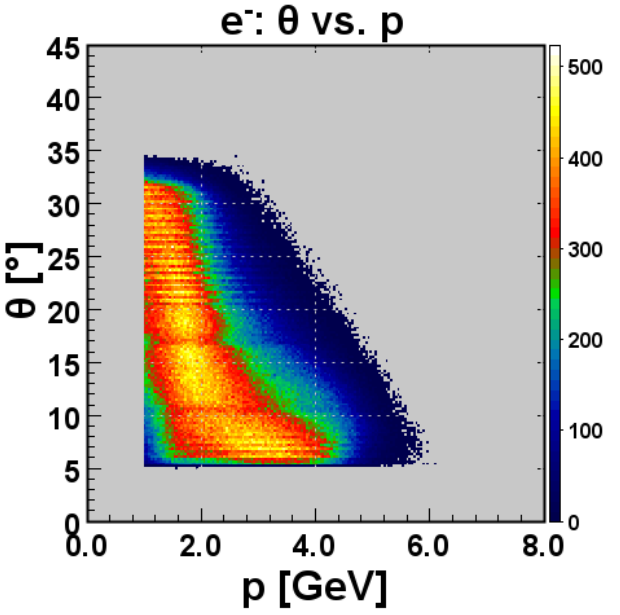

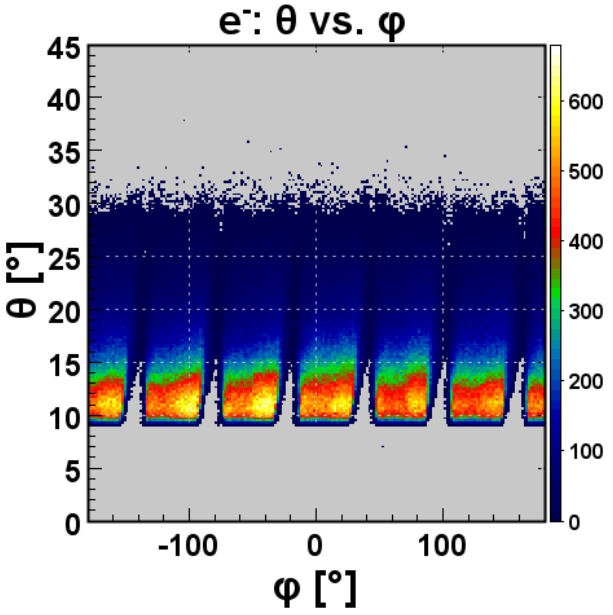

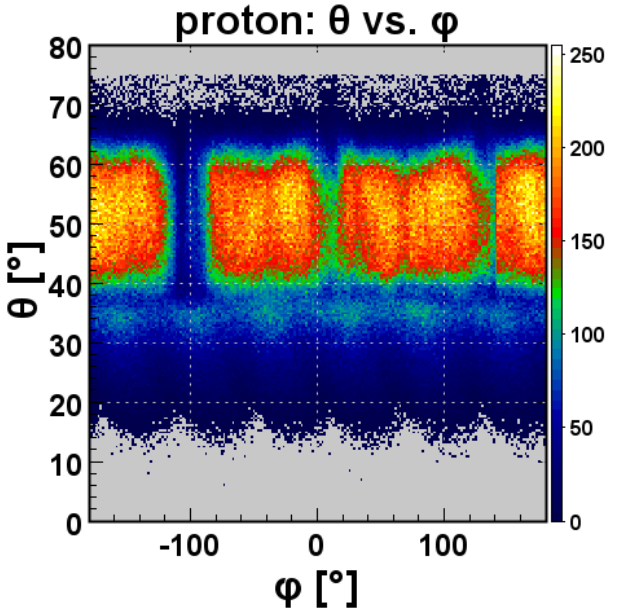

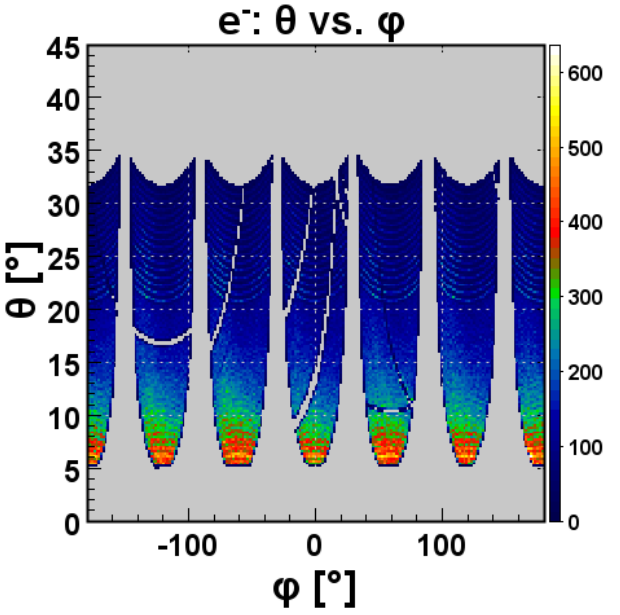

7.5 GeV Acceptance

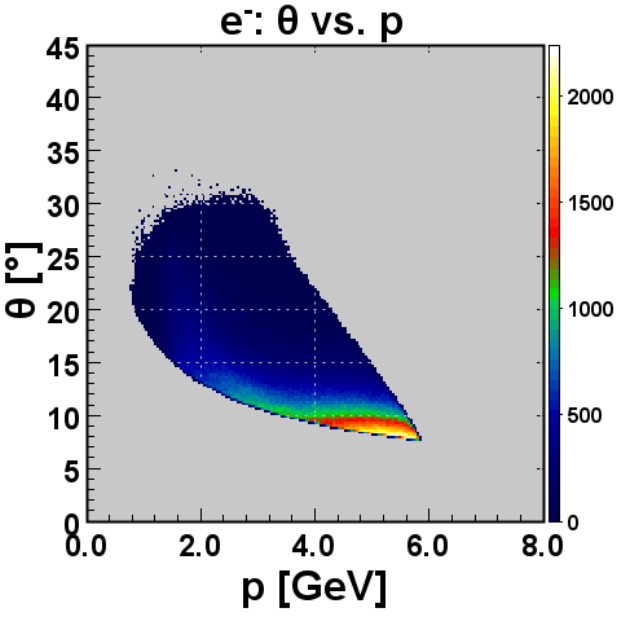

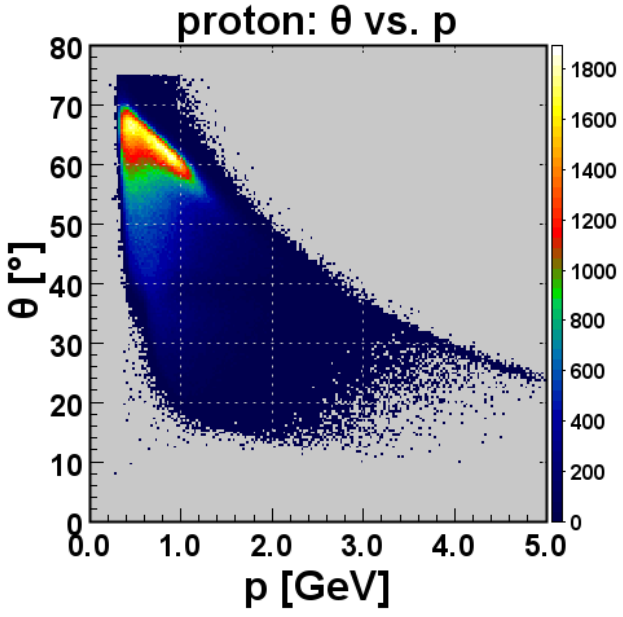

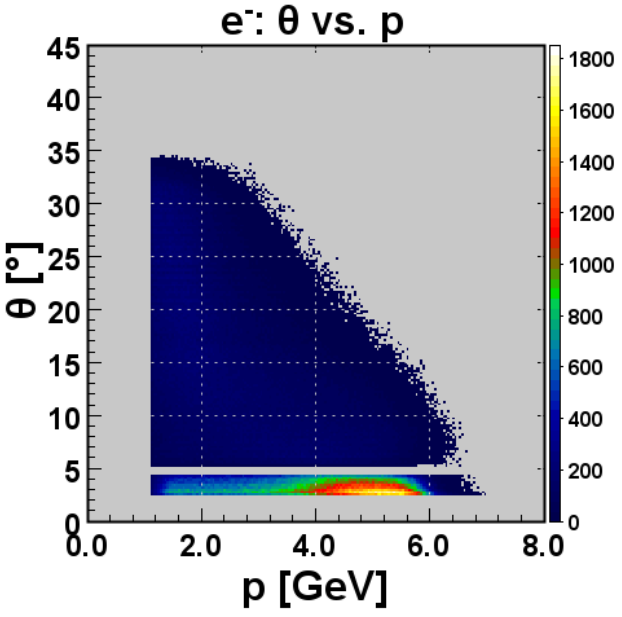

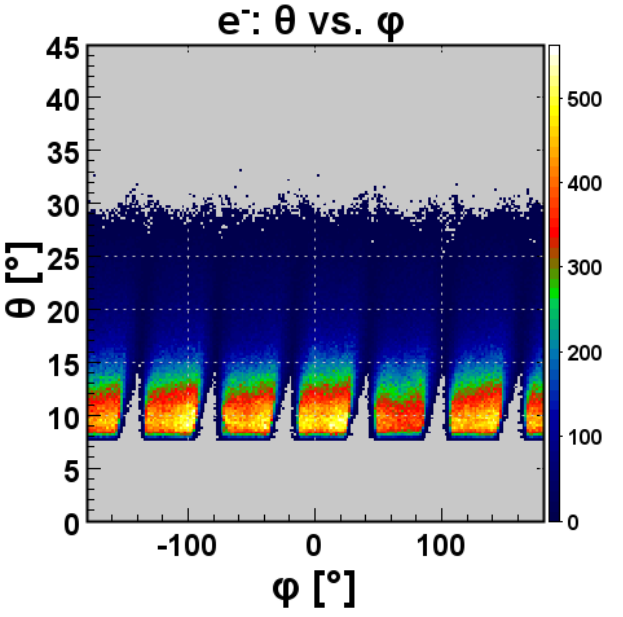

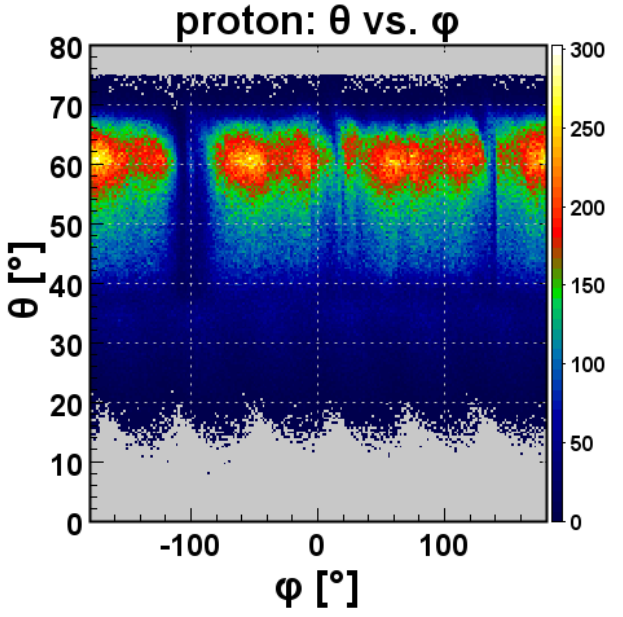

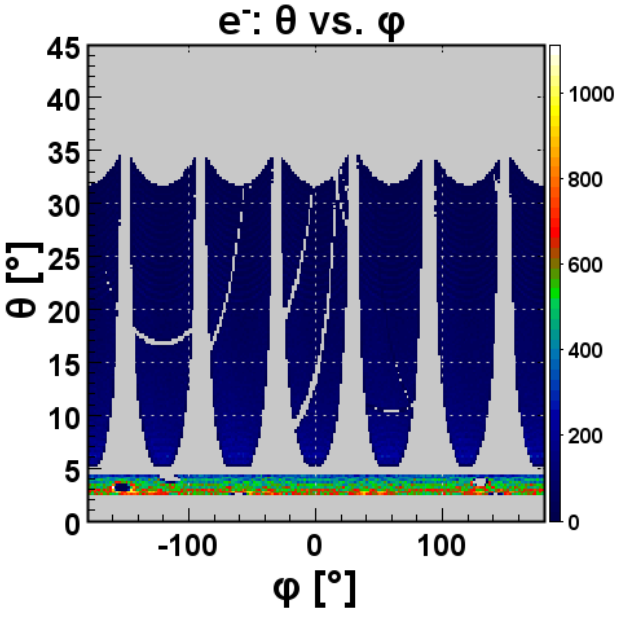

Q^2-x_B Bins

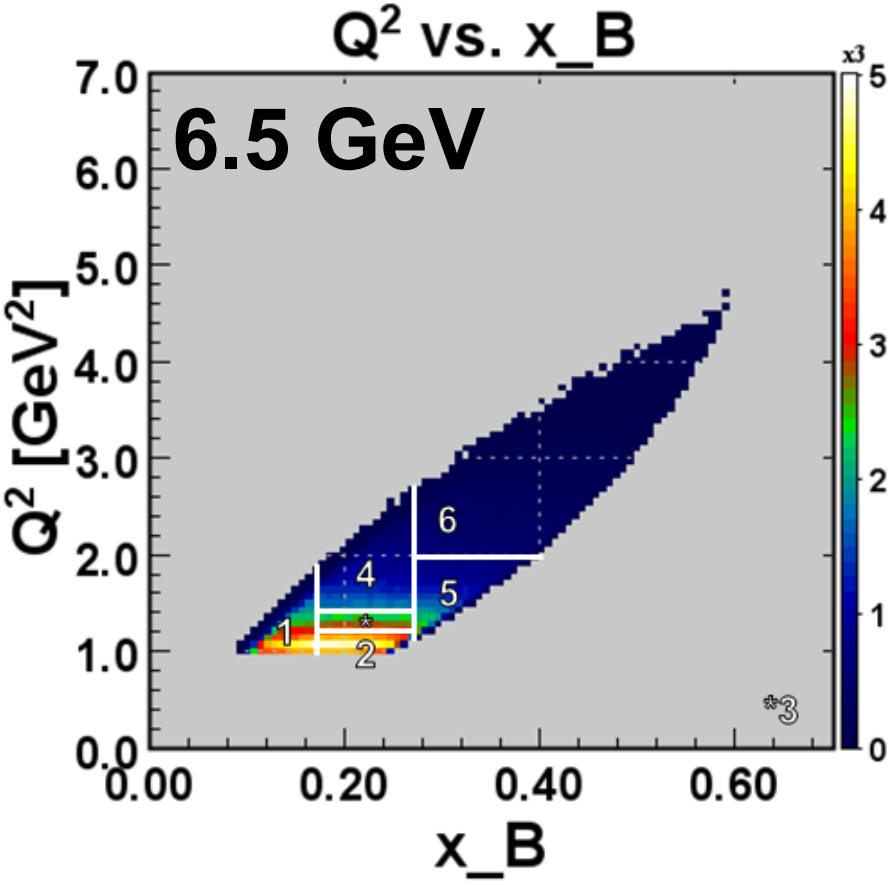

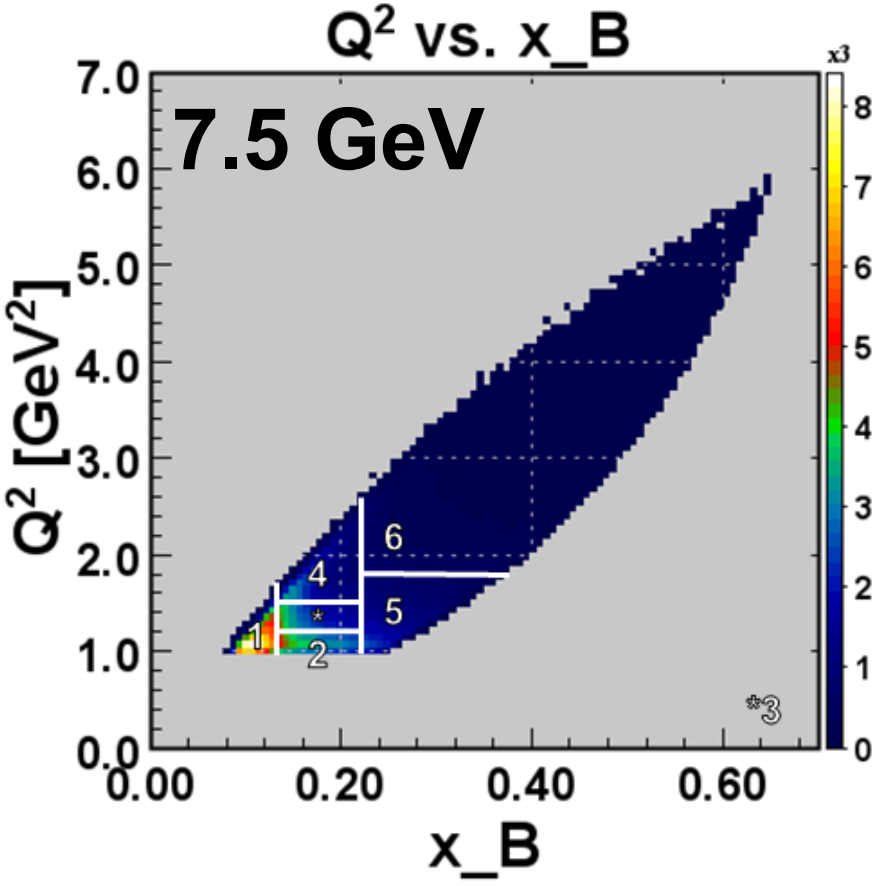

Bins were chosen to contain the same magnitude of the number of events.

6.5 GeV $-t$ Bins

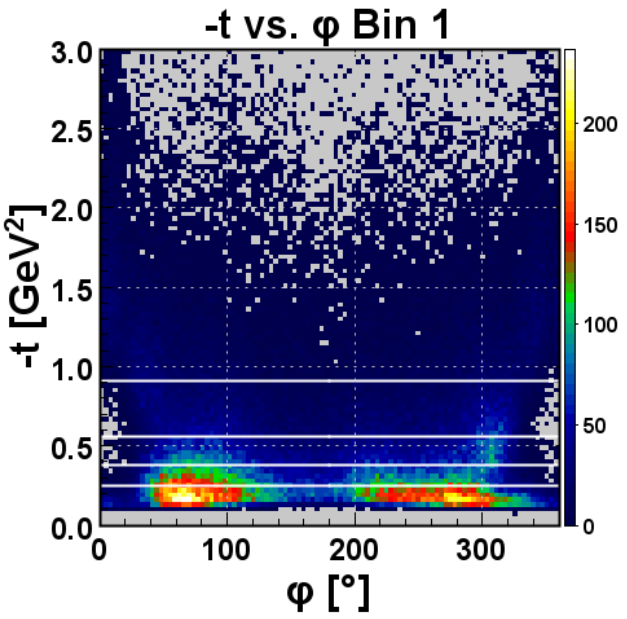
-t vs. φ Bin 1
-t [GeV²]
φ [°]

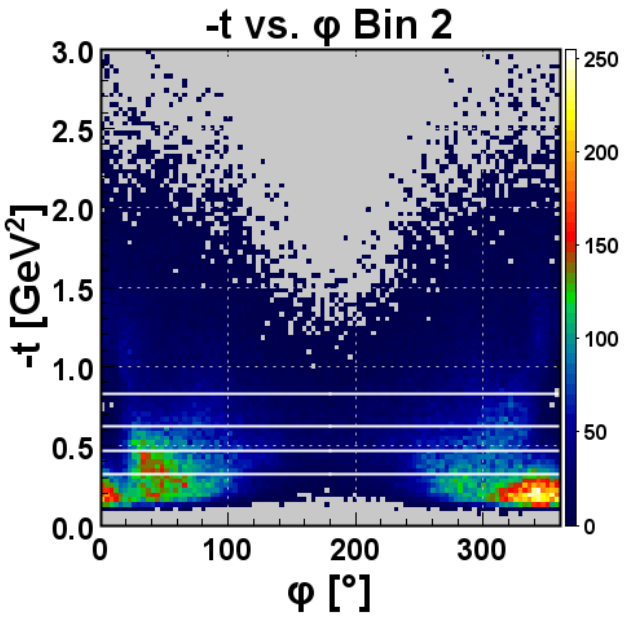
-t vs. φ Bin 2
-t [GeV²]
φ [°]

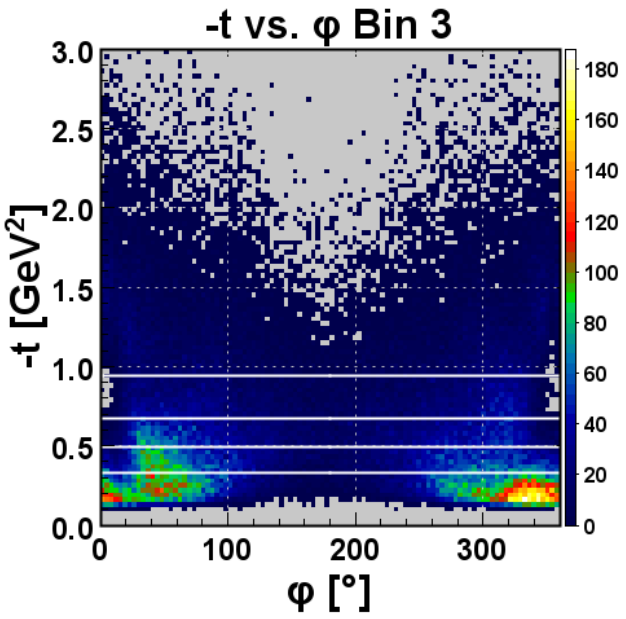
-t vs. φ Bin 3
-t [GeV²]
φ [°]

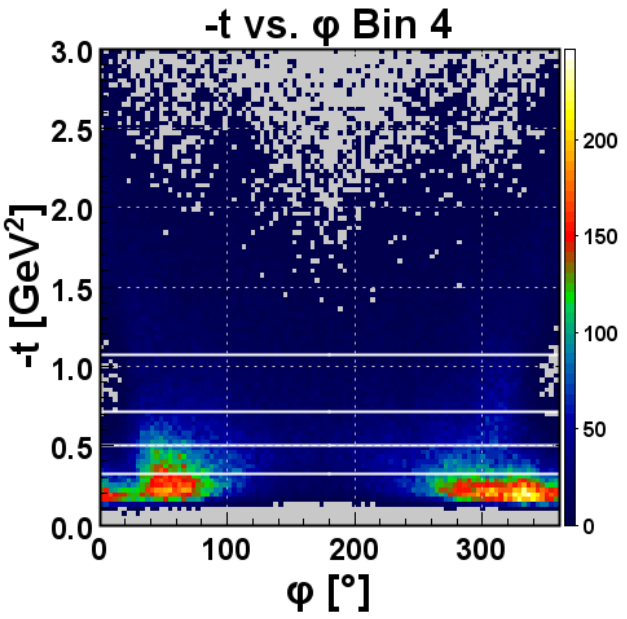
-t vs. φ Bin 4
-t [GeV²]
φ [°]

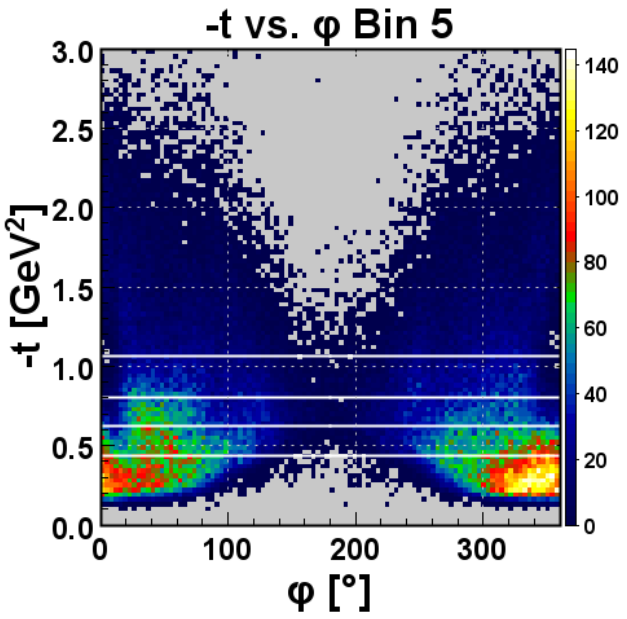
-t vs. φ Bin 5
-t [GeV²]
φ [°]

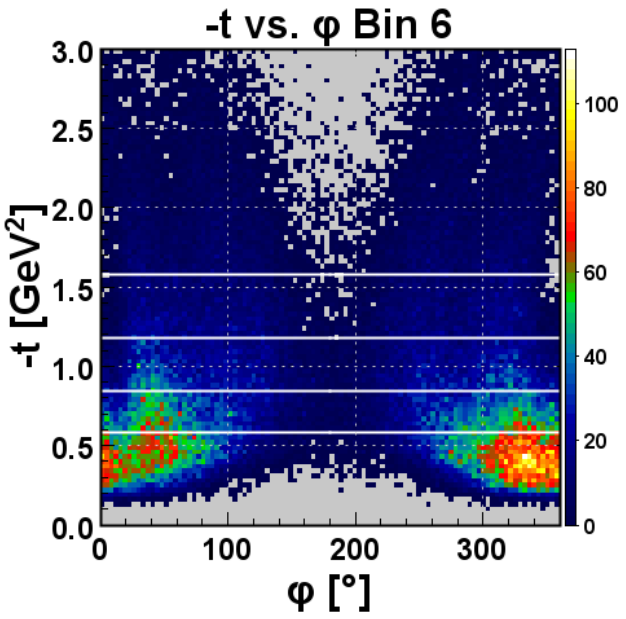
-t vs. φ Bin 6
-t [GeV²]
φ [°]

6.5 GeV Exclusivity Cuts

$$\Delta\theta = \cos^{-1}\frac{\overrightarrow{q'q'}_{\text{miss}}}{|\vec{q}||\overrightarrow{q'}_{\text{miss}}|}$$

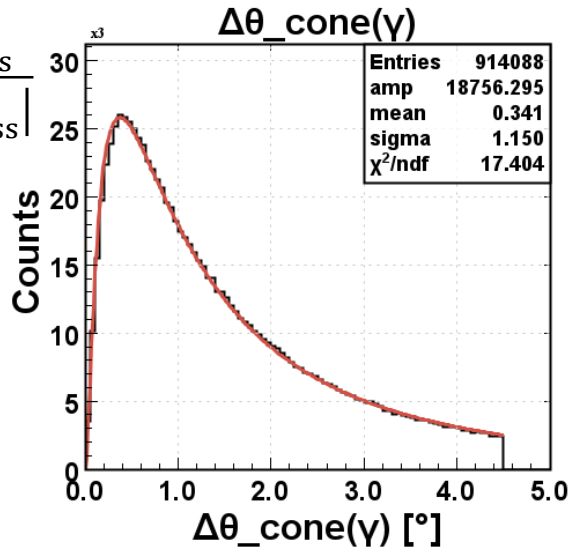

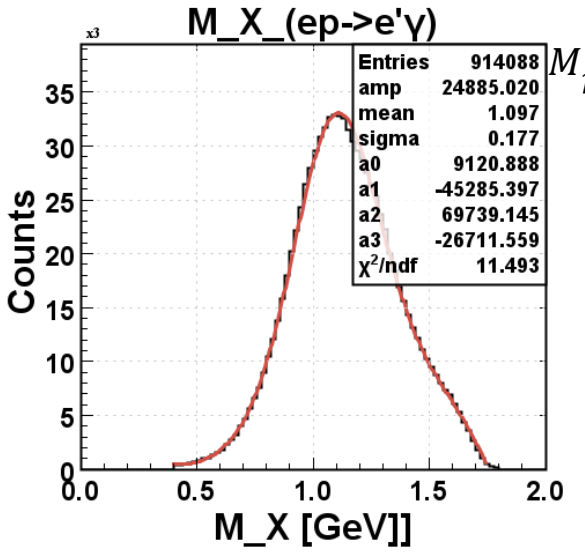

$M_{p'_{\text{miss}}} = \sqrt{p'_{\text{miss}} \cdot p'_{\text{miss}}}$

$X_{\text{miss}\perp}$

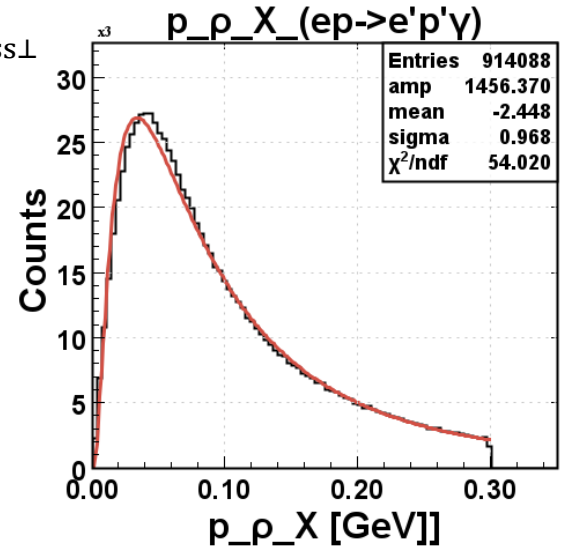

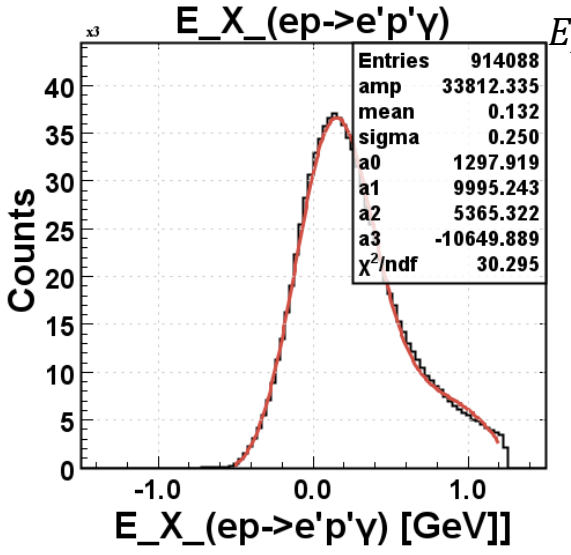

$E_{X_{\text{miss}}}$

Four kinematic cuts based on the exclusivity of the $ep \rightarrow e'p'\gamma X$ reaction, with X as the missing particle, were implemented.

6.5 GeV $\Delta\theta$ and $M_{p'_{\mathrm{miss}}}$ Cuts

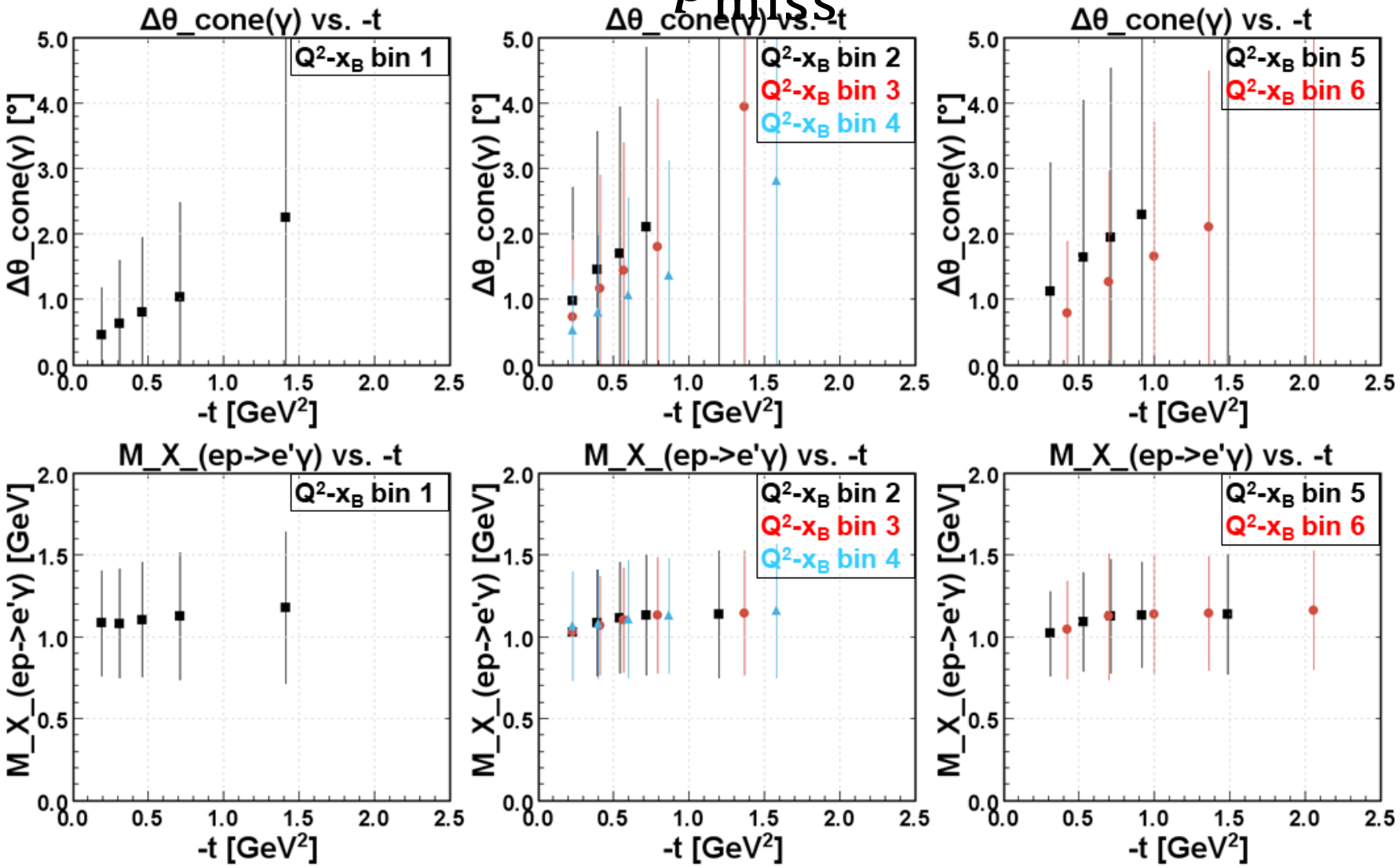

For each $(Q^2, x_B, -t)$ bin, $< e^{\mu+\sigma}$ cut was implemented for $\Delta\theta$ and $\mu \pm 2\sigma$ for $M_{p'_{\mathrm{miss}}}$.

6.5 GeV $X_{\mathrm{miss}\perp}$ and $E_{X_{\mathrm{miss}}}$ Cuts

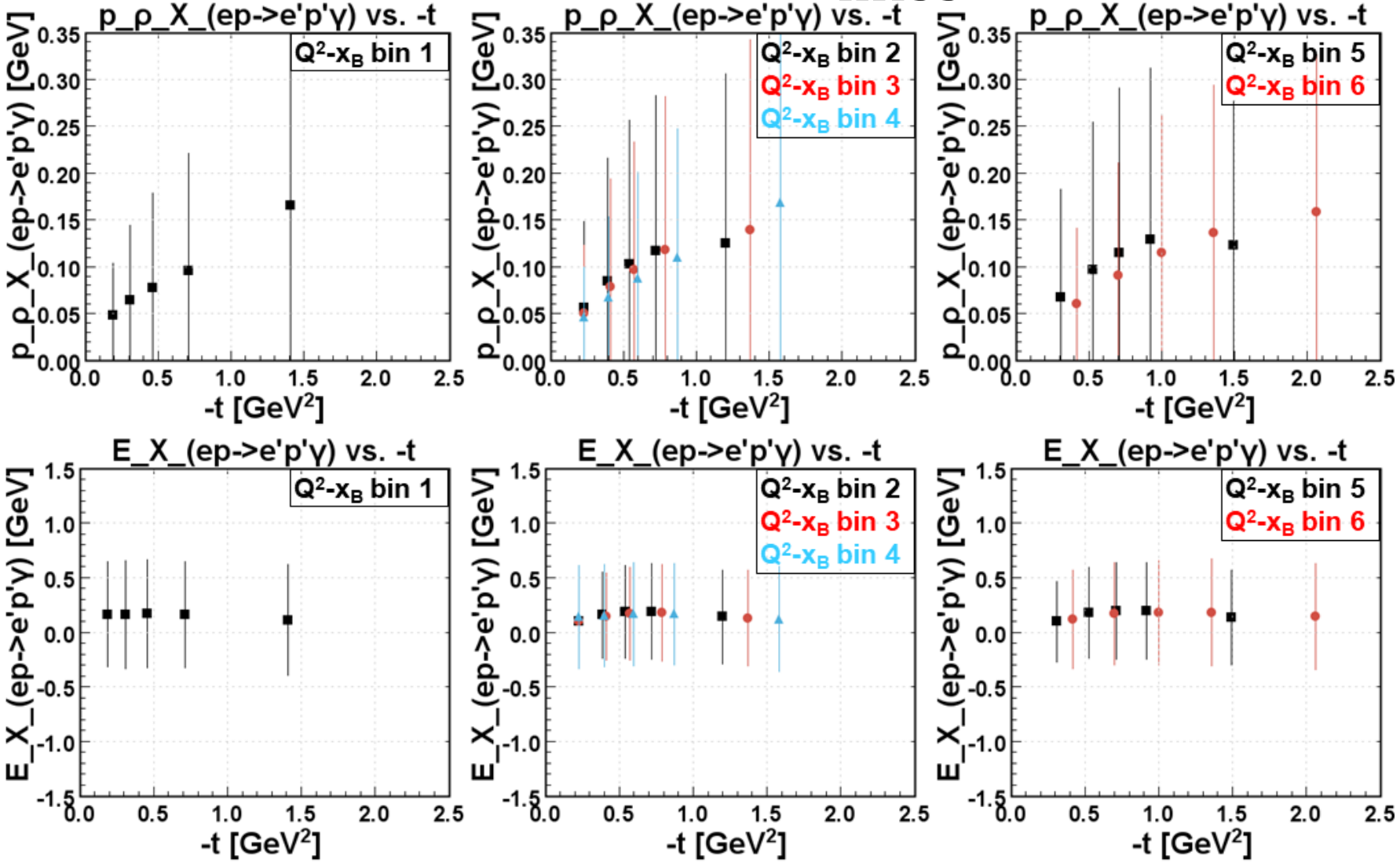

$(Q^2, x_B, -t)$-bin-dependent cuts of $< e^{\mu+\sigma}$ for $X_{\mathrm{miss}\perp}$ and $\mu \pm 2\sigma$ for $E_{X_{\mathrm{miss}}}$ were implemented.

7.5 $-t$ Bins

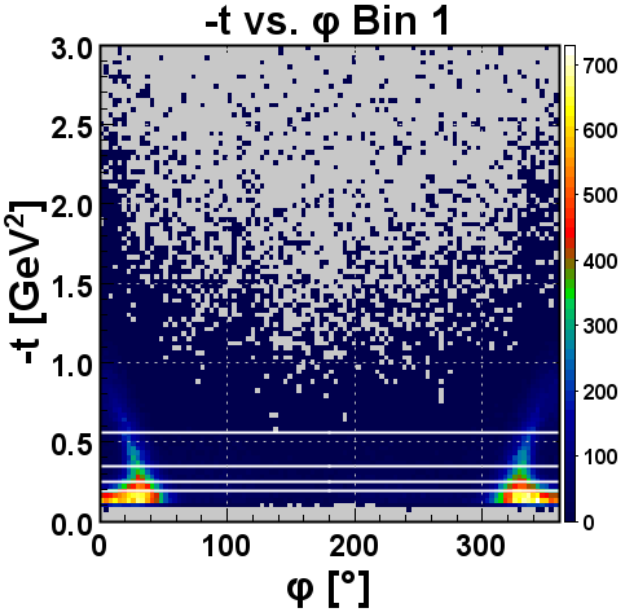
-t vs. φ Bin 1
-t [GeV²]
φ [°]

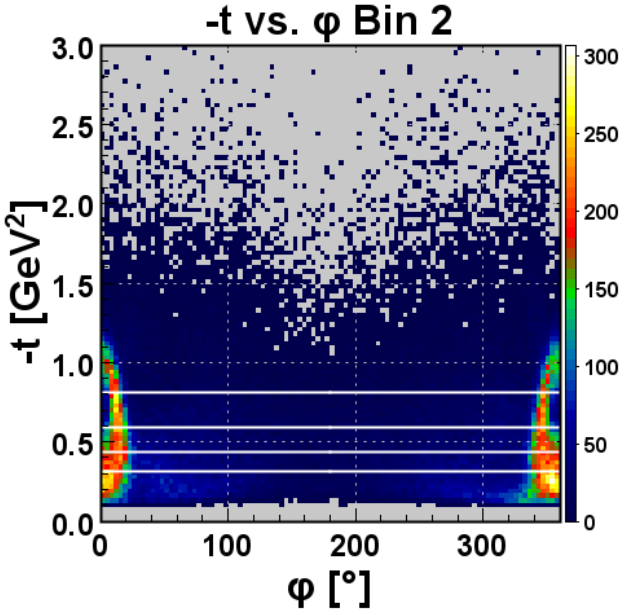
-t vs. φ Bin 2
-t [GeV²]
φ [°]

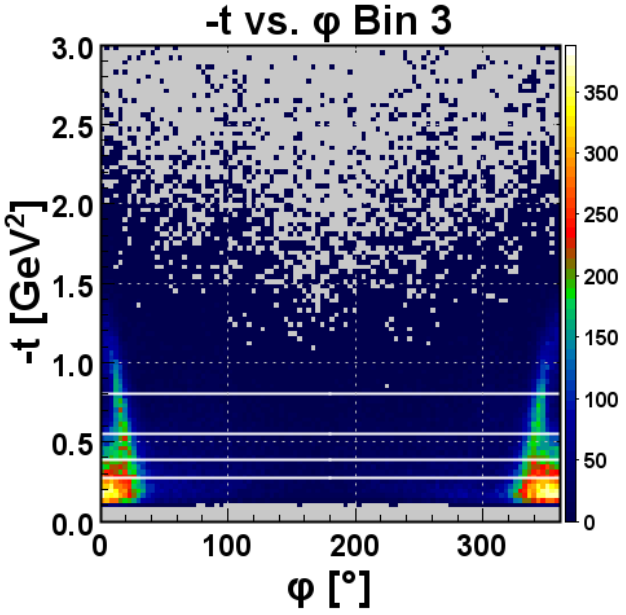
-t vs. φ Bin 3
-t [GeV²]
φ [°]

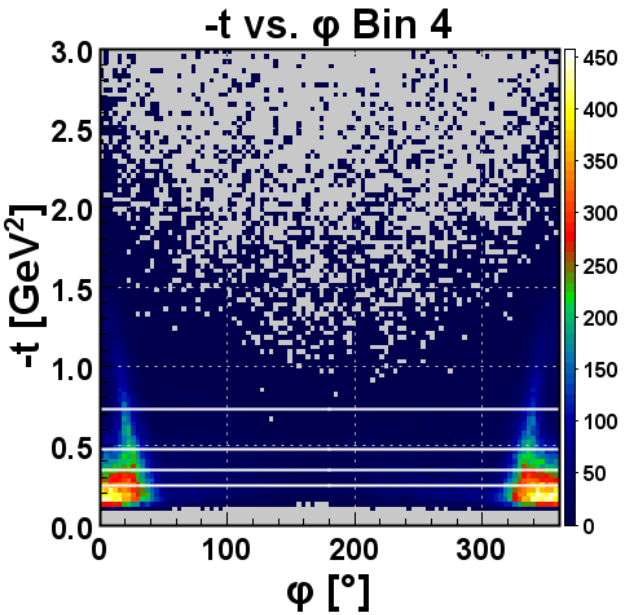
-t vs. φ Bin 4
-t [GeV²]
φ [°]

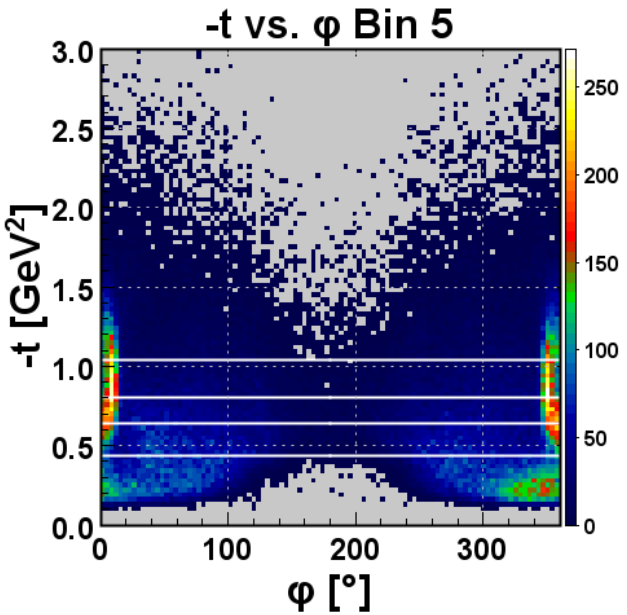
-t vs. φ Bin 5
-t [GeV²]
φ [°]

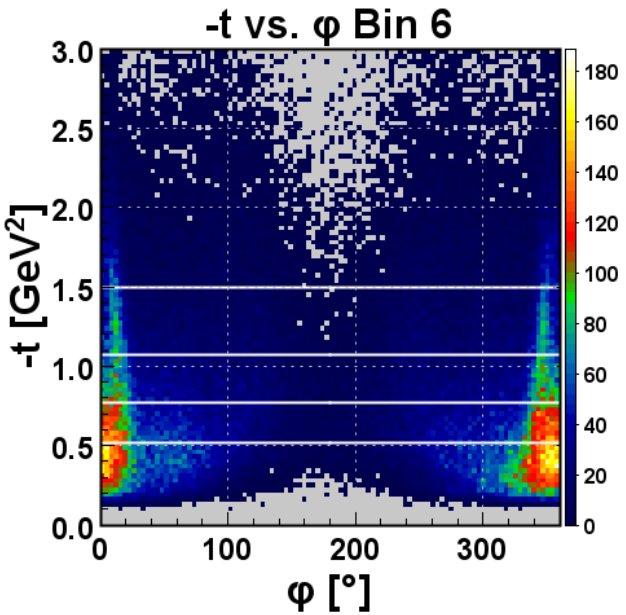
-t vs. φ Bin 6
-t [GeV²]
φ [°]

7.5 GeV ECal Exclusivity Cuts

$$\Delta\theta = \cos^{-1}\frac{\overrightarrow{q'q'}_{\text{miss}}}{|\vec{q}||\overrightarrow{q'}_{\text{miss}}|}$$

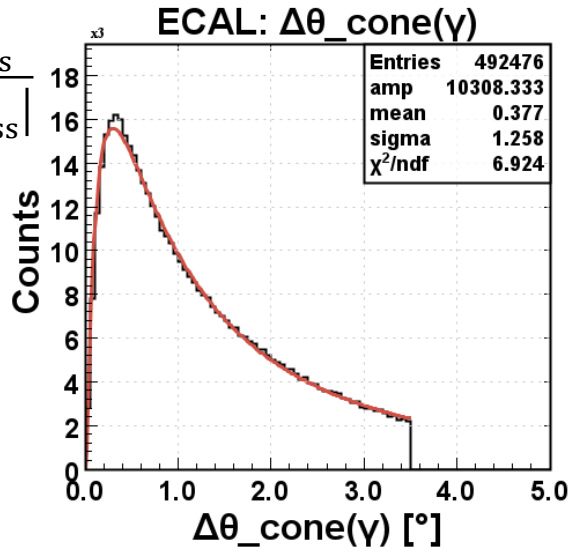

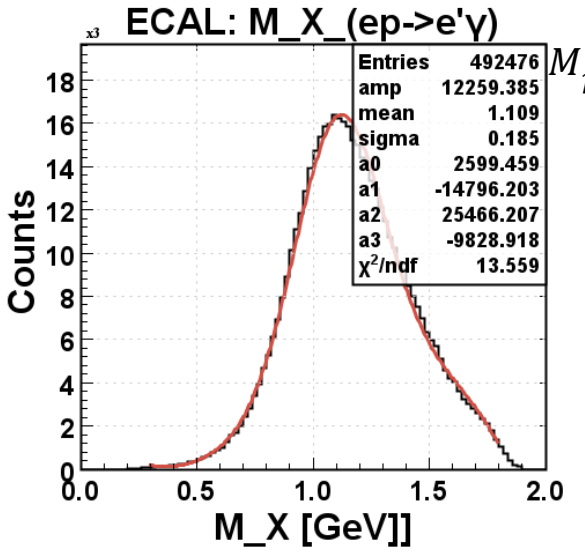

$$M_{p'_{\text{miss}}} = \sqrt{p'_{\text{miss}} \cdot p'_{\text{miss}}}$$

$X_{\text{miss}\perp}$

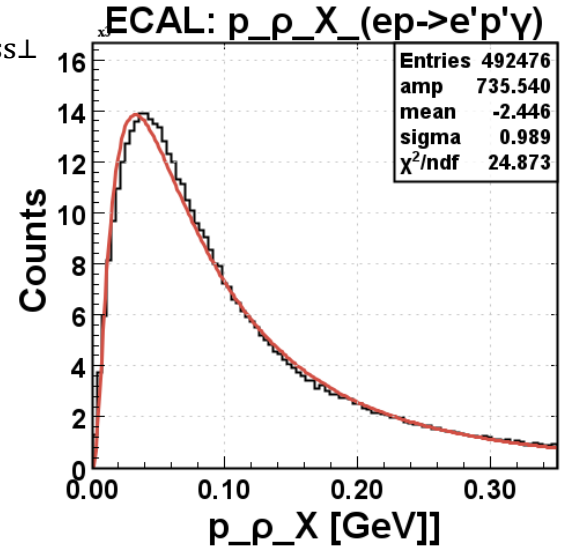

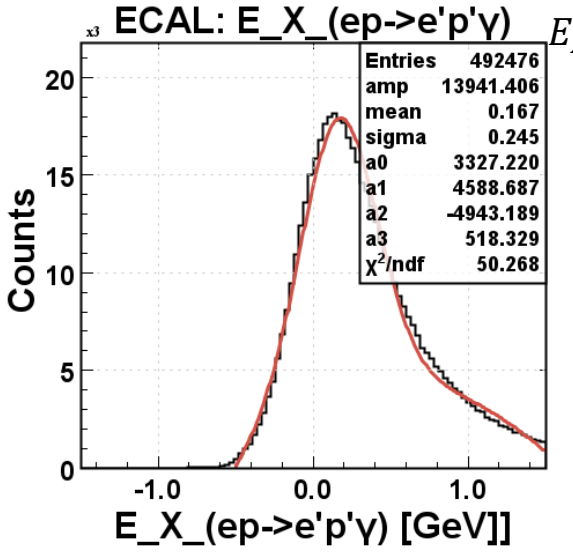

$E_{X_{\text{miss}}}$

Kinematic cuts based on $ep \rightarrow e'p'\gamma X$ reaction, with X as the missing particle and γ in ECal, were implemented.

7.5 GeV ECal $\Delta\theta$ and $M_{p'_{\mathrm{miss}}}$ Cuts

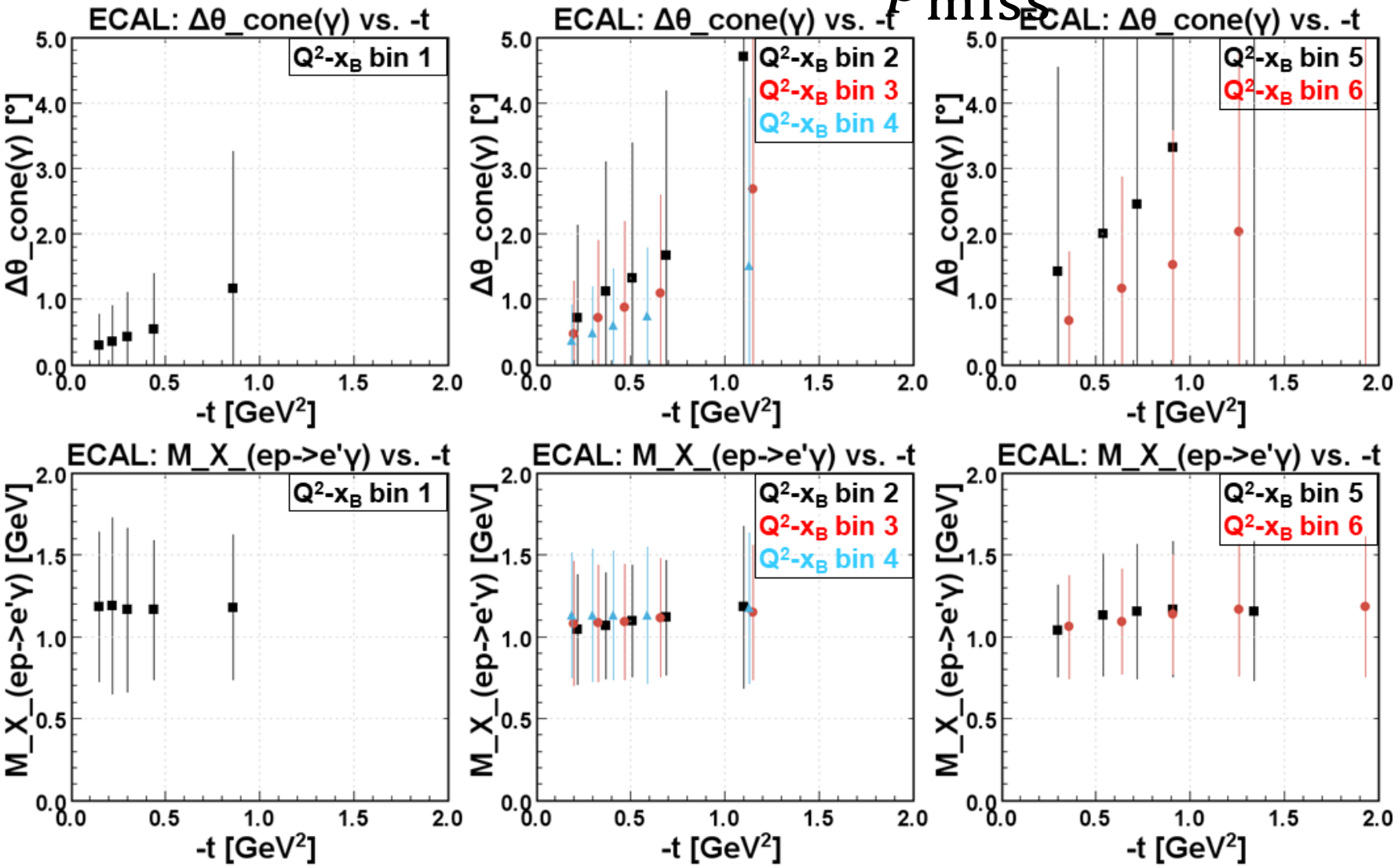

For each $(Q^2, x_B, -t)$ bin with γ in ECal, $< e^{\mu+\sigma}$ cut was implemented for $\Delta\theta$ and $\mu \pm 2\sigma$ for $M_{p'_{\mathrm{miss}}}$.

7.5 GeV ECal $X_{\mathrm{miss}\perp}$ and $E_{X_{\mathrm{miss}}}$ Cuts

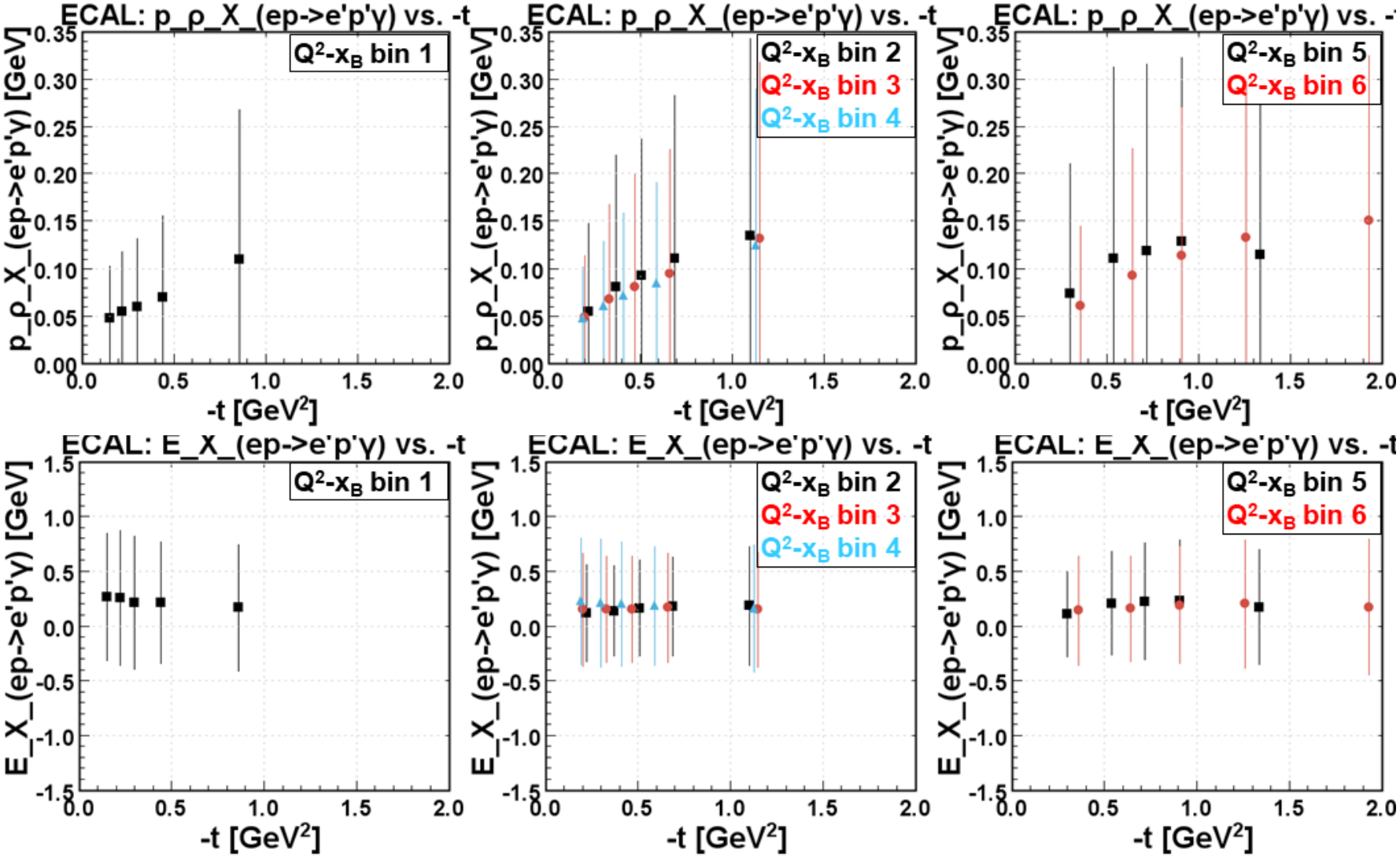

$(Q^2, x_B, -t)$-bin-dependent cuts of $< e^{\mu+\sigma}$ for $X_{\mathrm{miss}\perp}$ and $\mu \pm 2\sigma$ for $E_{X_{\mathrm{miss}}}$ were implemented to events with γ in ECal.

7.5 GeV FTCal Exclusivity Cuts

$$\Delta\theta = \cos^{-1}\frac{\overrightarrow{q'q'}_{\text{miss}}}{|\vec{q}||\overrightarrow{q'}_{\text{miss}}|}$$

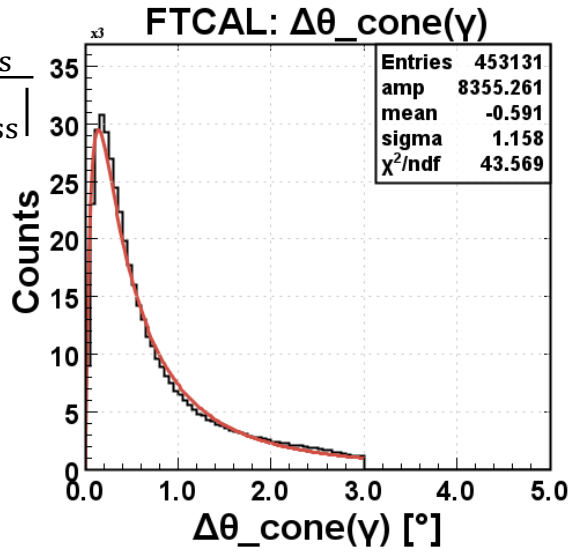

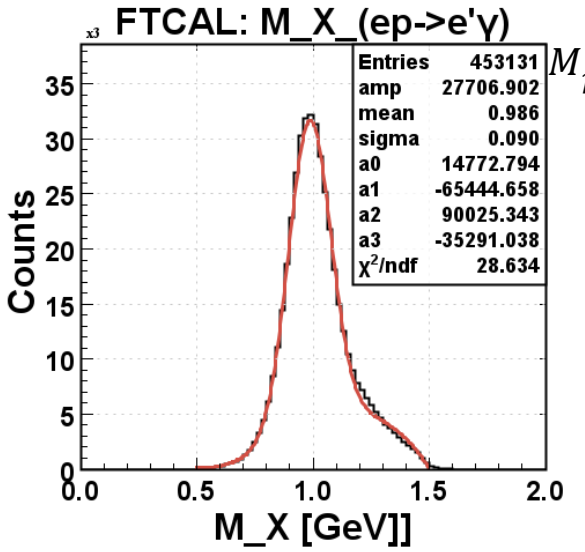

$M_{p'_{\text{miss}}} = \sqrt{p'_{\text{miss}} \cdot p'_{\text{miss}}}$

$X_{\text{miss}\perp}$

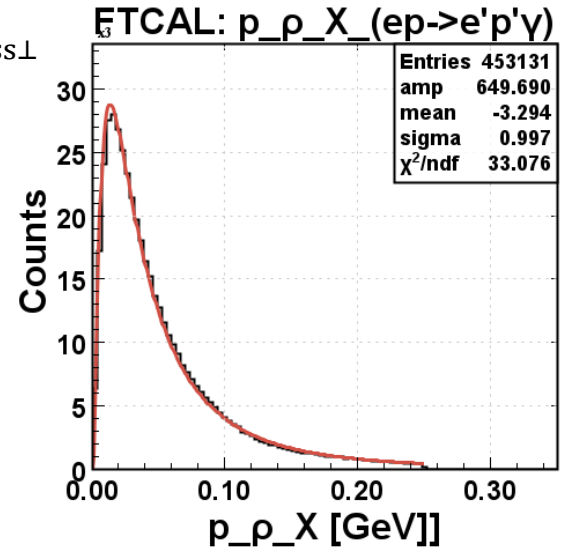

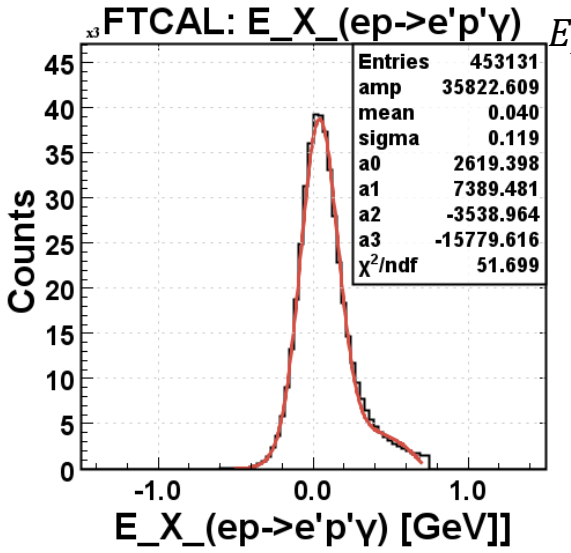

$E_{X_{\text{miss}}}$

Same cuts based on $ep \to e'p'\gamma X$ reaction, with X as the missing particle but with γ in FTCal, were implemented.

7.5 GeV FTCal $\Delta\theta$ and $M_{p'_{\mathrm{miss}}}$ Cuts

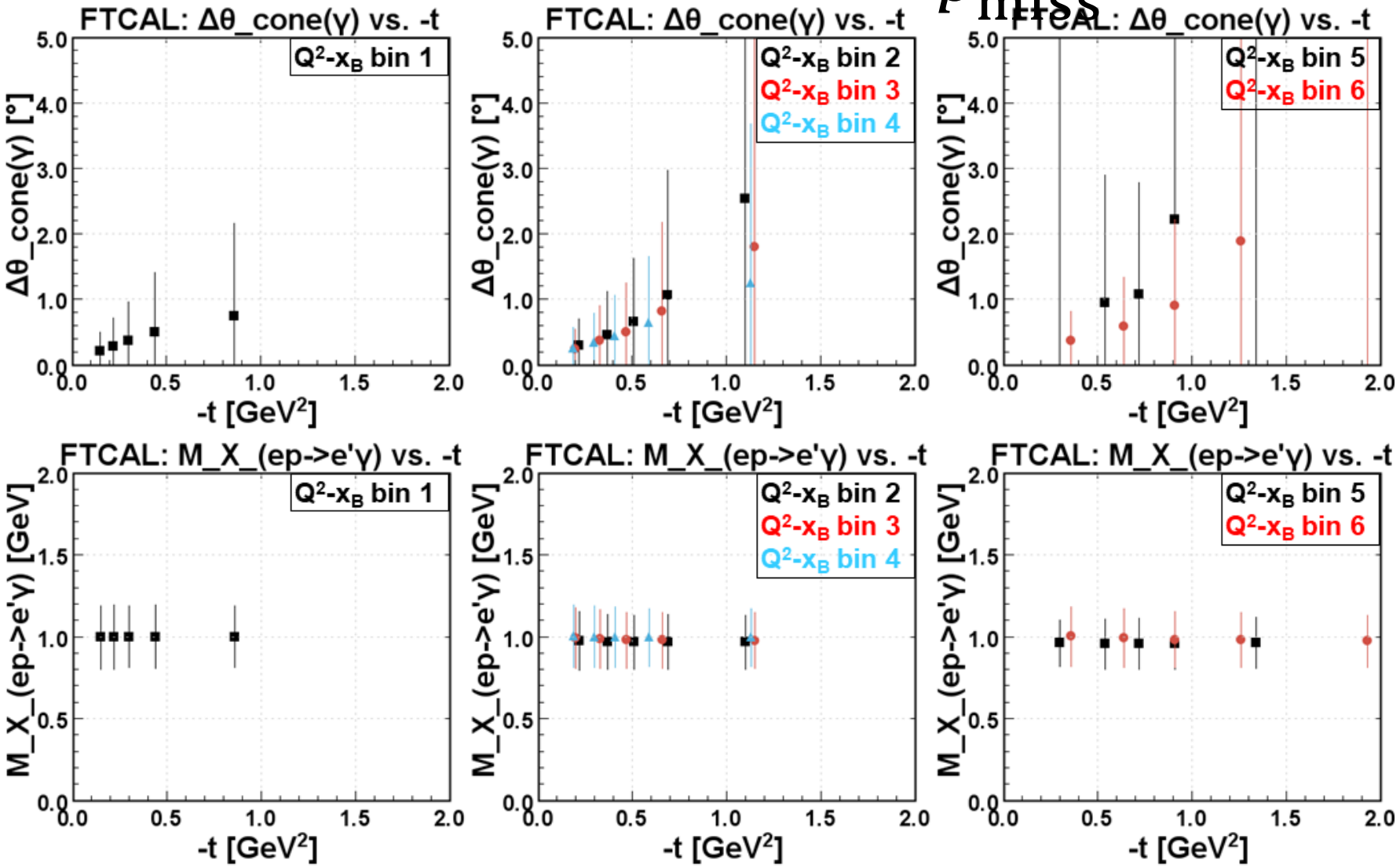

For each $(Q^2, x_B, -t)$ bin with γ in FTCal, $< e^{\mu+\sigma}$ cut was implemented for $\Delta\theta$ and $\mu \pm 2\sigma$ for $M_{p'_{\mathrm{miss}}}$.

7.5 GeV FTCal $X_{\mathrm{miss}\perp}$ and $E_{X_{\mathrm{miss}}}$ Cuts

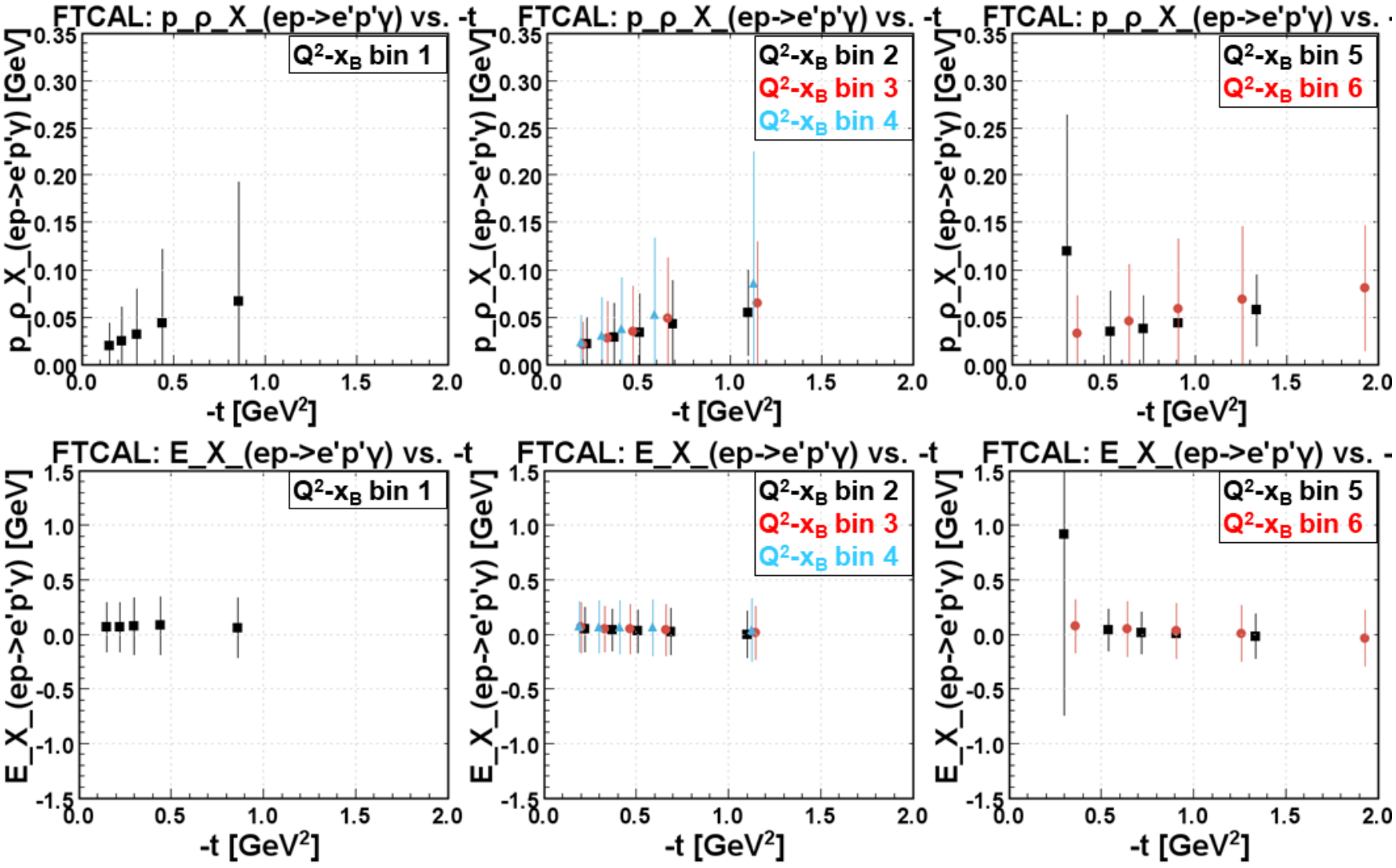

$(Q^2, x_B, -t)$-bin-dependent cuts of $< e^{\mu+\sigma}$ for $X_{\mathrm{miss}\perp}$ and $\mu \pm 2\sigma$ for $E_{X_{\mathrm{miss}}}$ were implemented to events with γ in FTCal.

Raw Beam Spin Asymmetry

Integrated Raw BSA

$$A = \frac{\alpha \sin\phi}{1 + \beta \cos\phi}$$

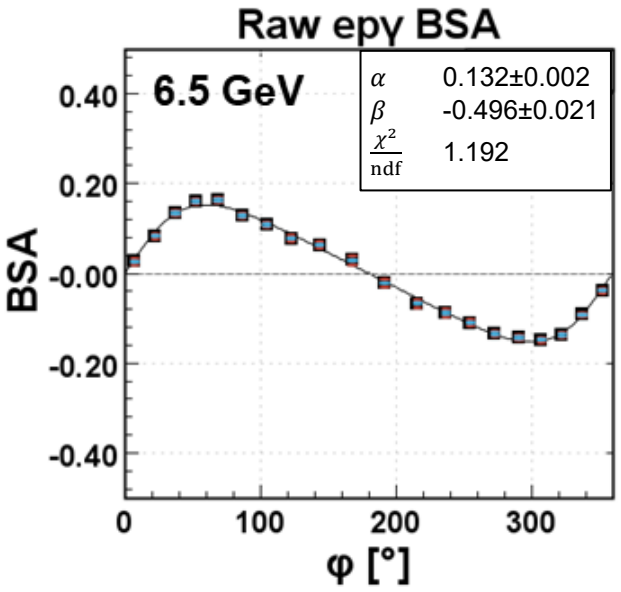

$$A = \frac{\alpha \sin\phi}{1 + \beta \cos\phi}$$

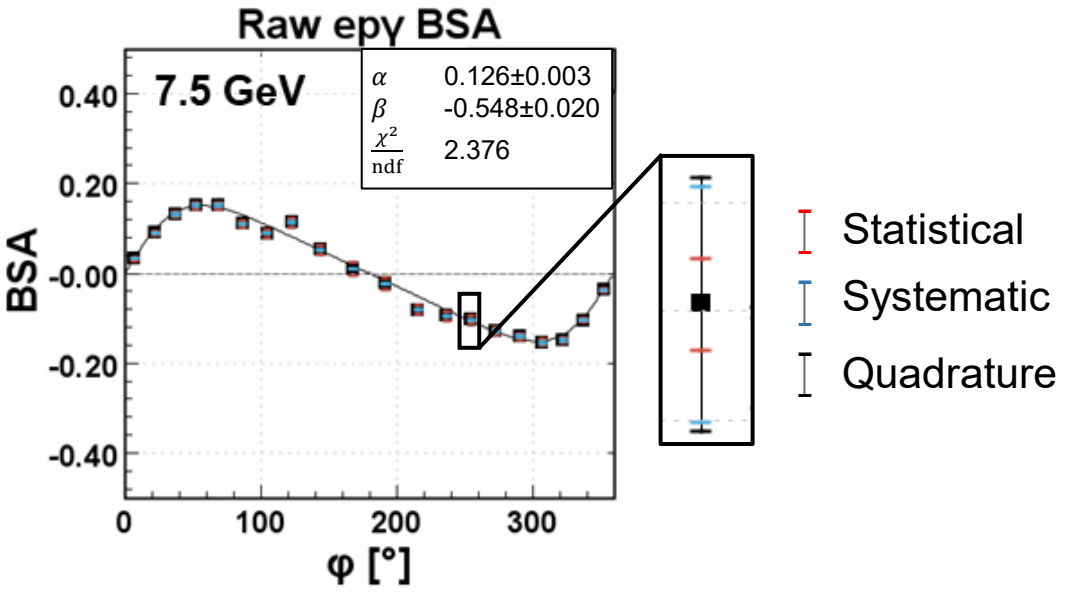

Raw BSA includes BSA contribution from DVπ^0P events detected with only one γ.

6.5 GeV Raw BSA α

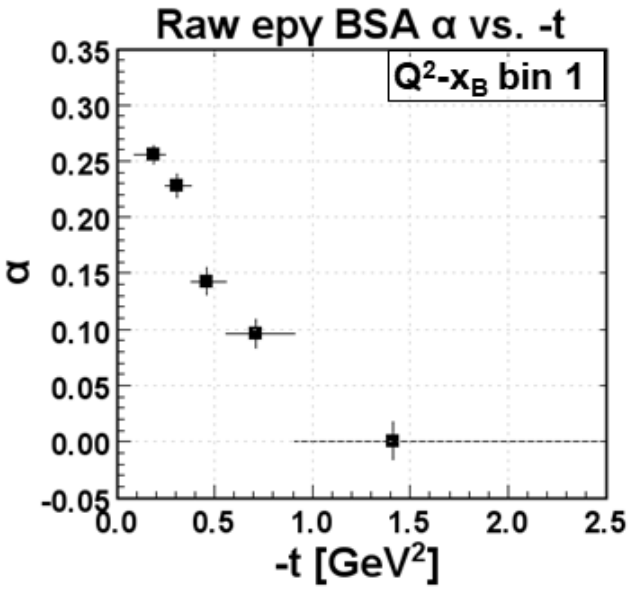

x_B < 0.17

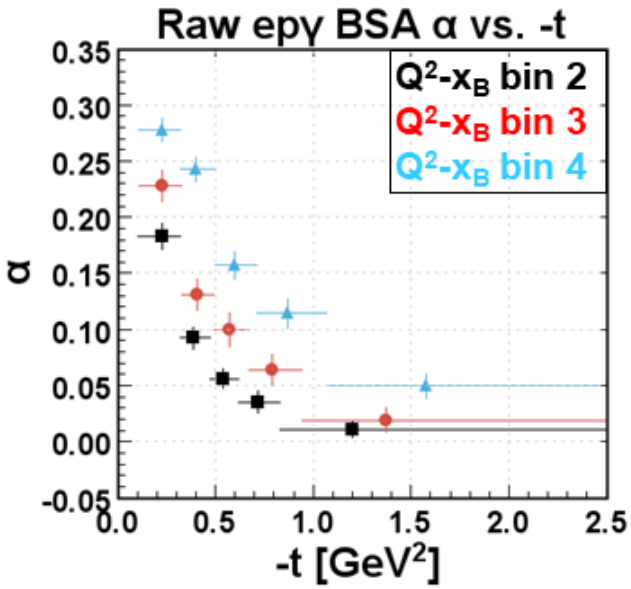

0.17 ≤ x_B < 0.27 :
Q^2 < 1.2 GeV²
1.2 GeV² ≤ Q^2 < 1.4 GeV²
1.4 GeV² ≤ Q^2

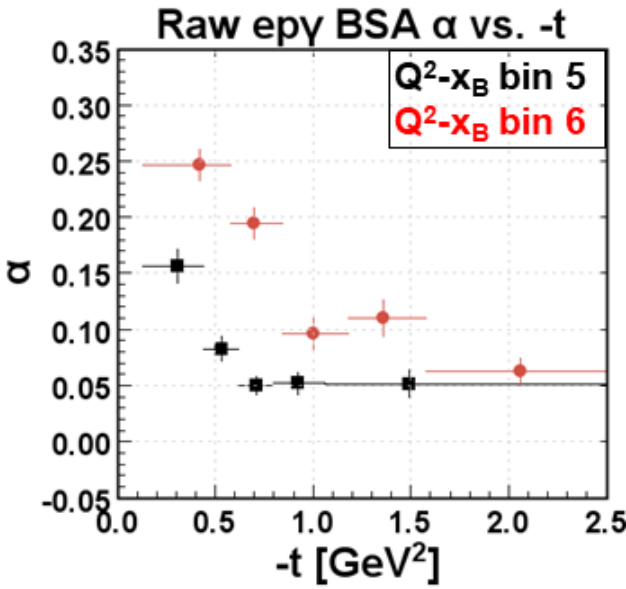

0.27 ≤ x_B :
Q^2 < 2.0 GeV²
2.0 GeV² ≤ Q^2

Raw BSA α also includes contribution from DVπ^0P events detected with only one γ.

7.5 GeV Raw BSA α

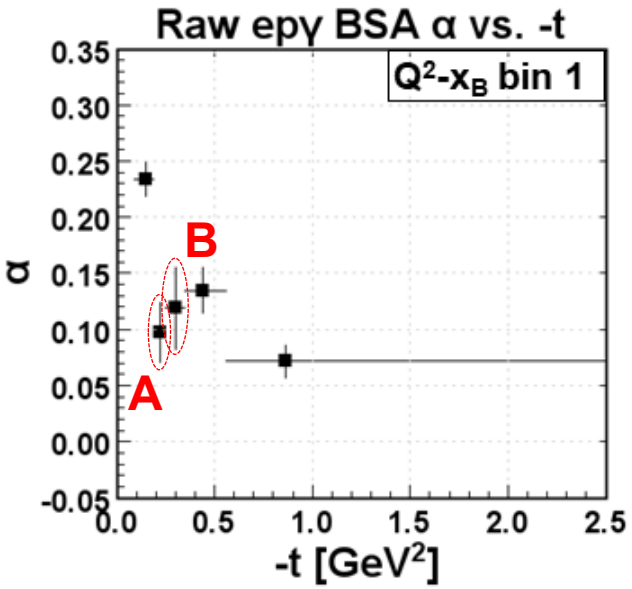

x_B < 0.13

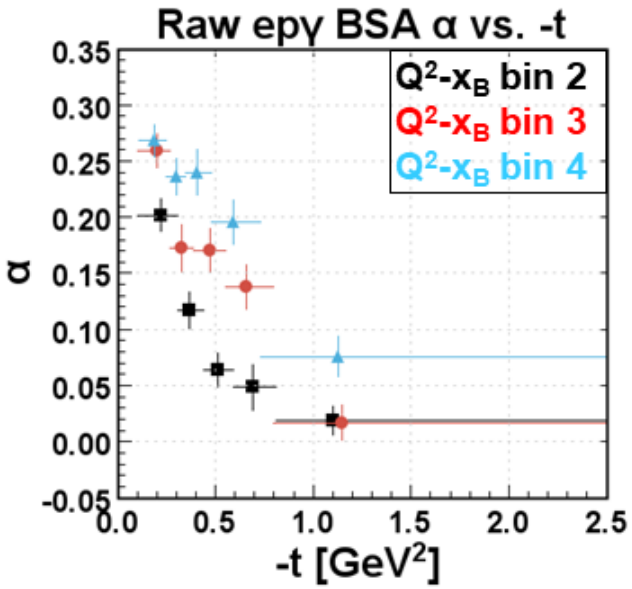

0.13 ≤ x_B < 0.22 :
Q^2 < 1.2 GeV²
1.2 GeV² ≤ Q^2 < 1.5 GeV²
1.5 GeV² ≤ Q^2

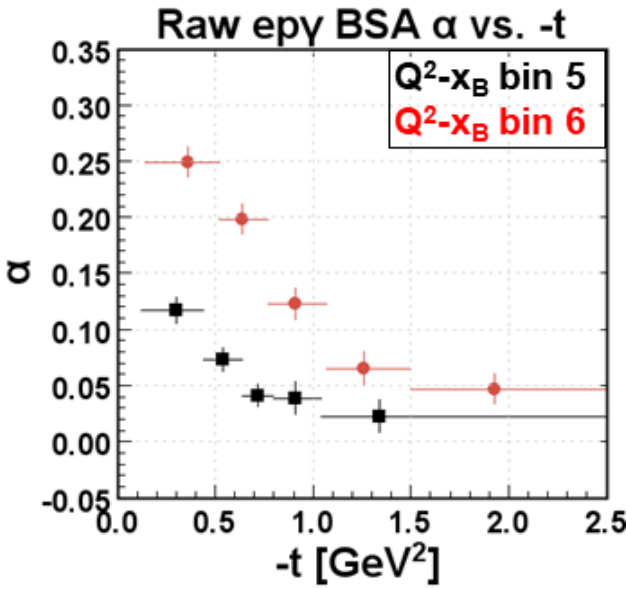

0.22 ≤ x_B :
Q^2 < 1.8 GeV²
1.8 GeV² ≤ Q^2

"Out-of-trend" measurements can be distinguished even at the early stage of BSA α (**A** and **B**) extraction.

DVπ^0P Contamination Subtraction

$ep \to e'p'(\gamma\gamma_{\mathrm{miss}})_{\pi^0}$ Contaminants

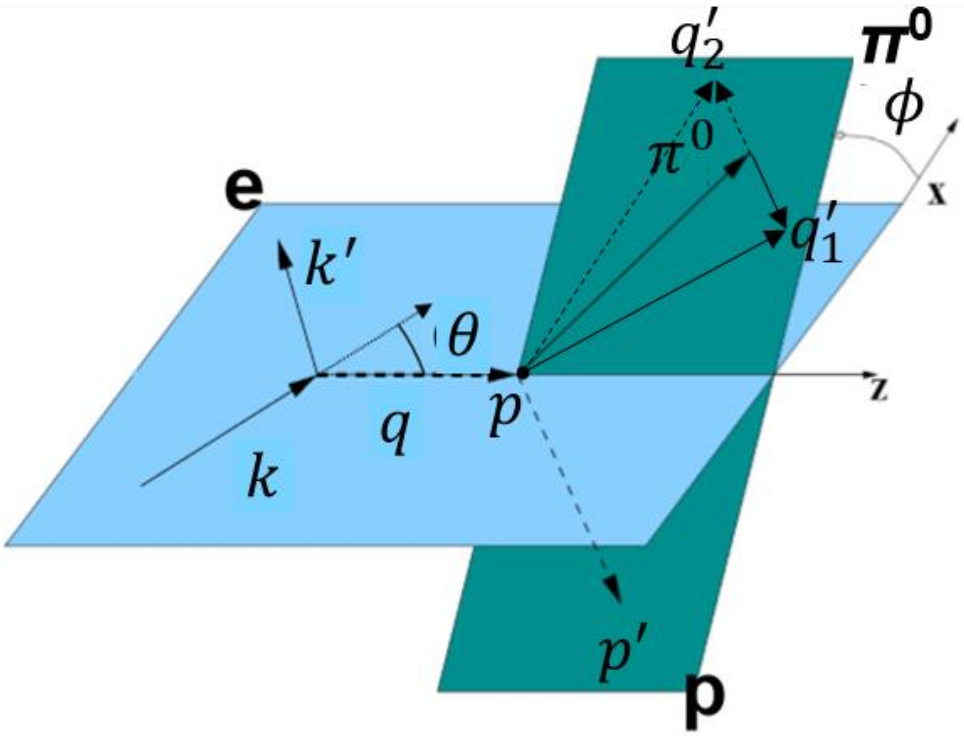

$$r = \left.\frac{N_{\pi^0(\gamma)}}{N_{\pi^0(\gamma\gamma)}}\right|_{\mathrm{dat}} = \left.\frac{N_{\pi^0(\gamma)}}{N_{\pi^0(\gamma\gamma)}}\right|_{\mathrm{sim}}$$

$$f = r\frac{N_{\pi^0(\gamma\gamma)}}{N_{ep\gamma}}$$

$$A = \frac{1}{1-f}\left(A_{ep\gamma} - fA_{\pi^0(\gamma\gamma)}\right)$$

Exclusive DVπ^0P event is misidentified as DVCS when one of its final-state photons (γ_{miss}) has sufficiently low energy and lands outside the detector's acceptance.

6.5 GeV DVπ^0P Cuts

$$\Delta\theta = \cos^{-1}\frac{\overrightarrow{\pi^0}\overrightarrow{\pi^0}_{\text{miss}}}{\left|\overrightarrow{\pi^0}\right|\left|\overrightarrow{\pi^0}_{\text{miss}}\right|}$$

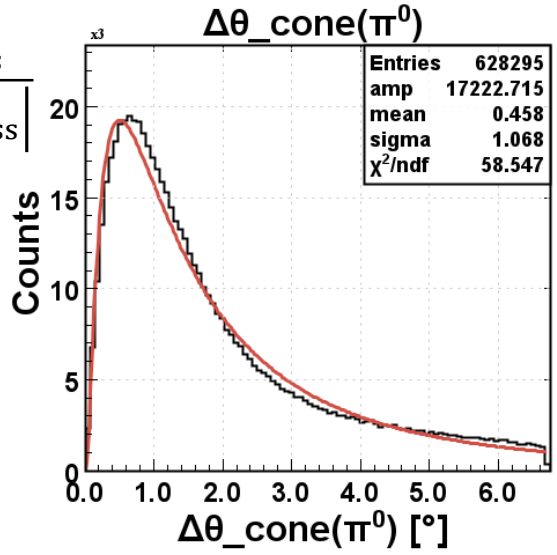

$M_{p'_{\text{miss}}} = \sqrt{p'_{\text{miss}} \cdot p'_{\text{miss}}}$

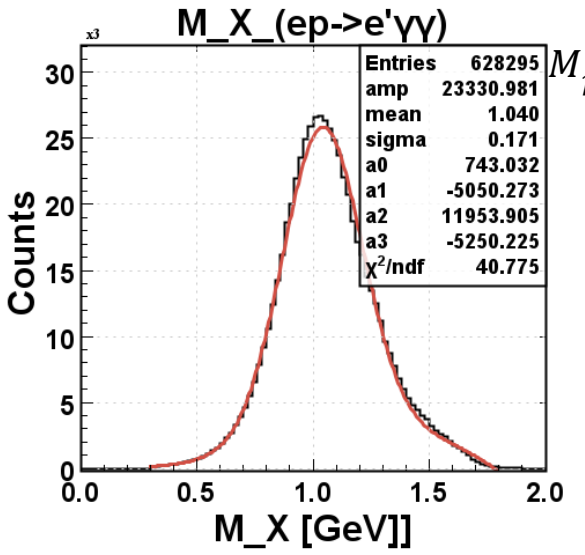

$X_{\text{miss}\perp}$

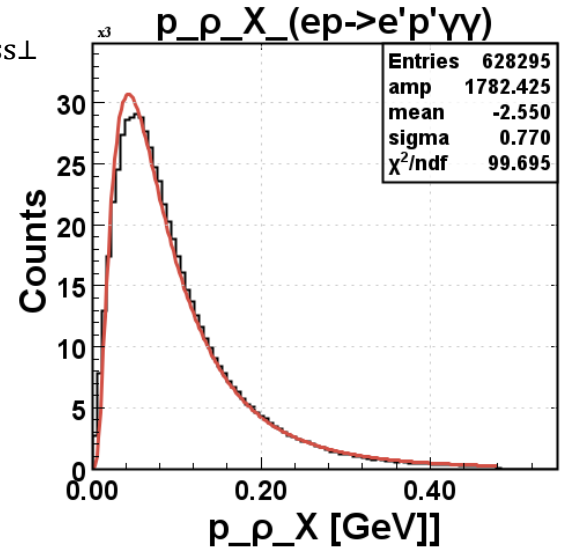

$E_{X_{\text{miss}}}$

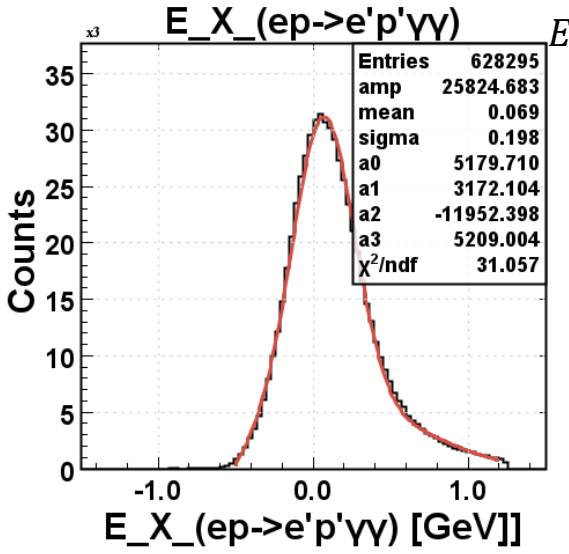

The kinematic cuts were adopted based on the exclusivity of the $ep \rightarrow e'p'(\gamma\gamma)_{\pi^0}X$ reaction.

7.5 GeV ECal-ECal Cuts

$$\Delta\theta = \cos^{-1}\frac{\overrightarrow{\pi^0}\overrightarrow{\pi^0}_{\text{miss}}}{\left|\overrightarrow{\pi^0}\right|\left|\overrightarrow{\pi^0}_{\text{miss}}\right|}$$

$$M_{p'_{\text{miss}}} = \sqrt{p'_{\text{miss}} \cdot p'_{\text{miss}}}$$

$$X_{\text{miss}\perp}$$

$$E_{X_{\text{miss}}}$$

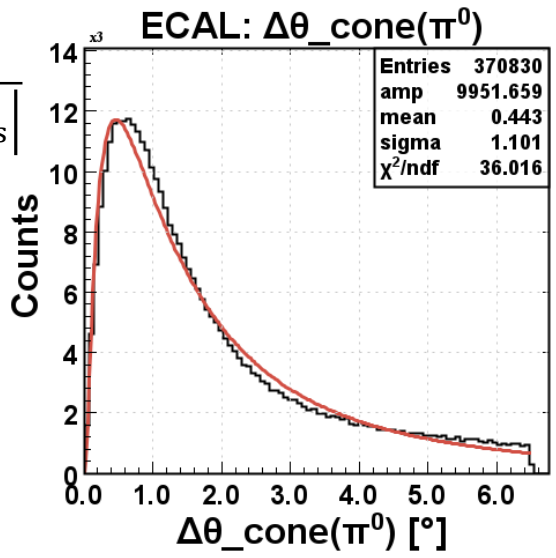

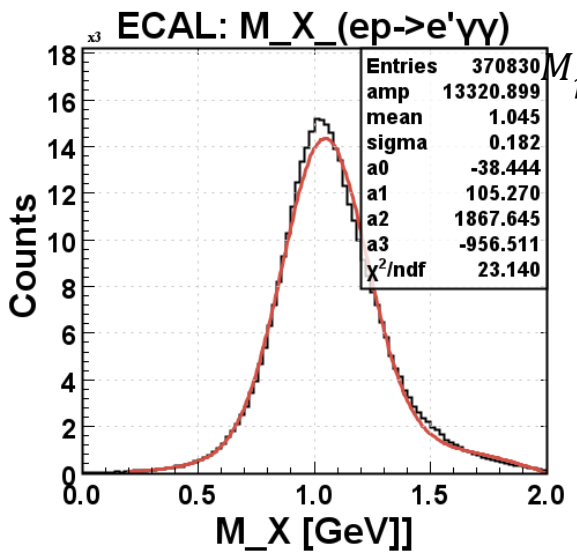

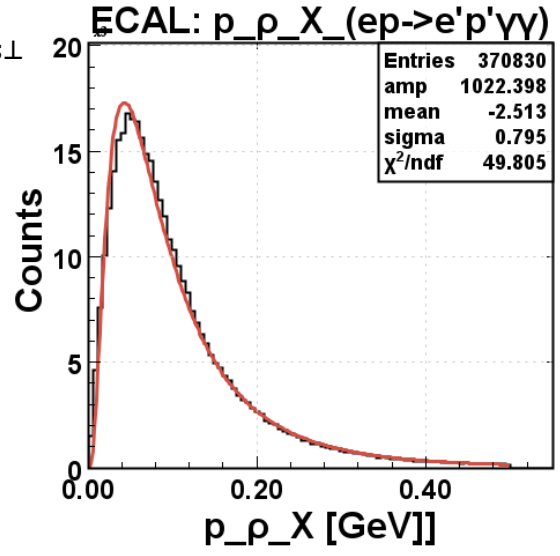

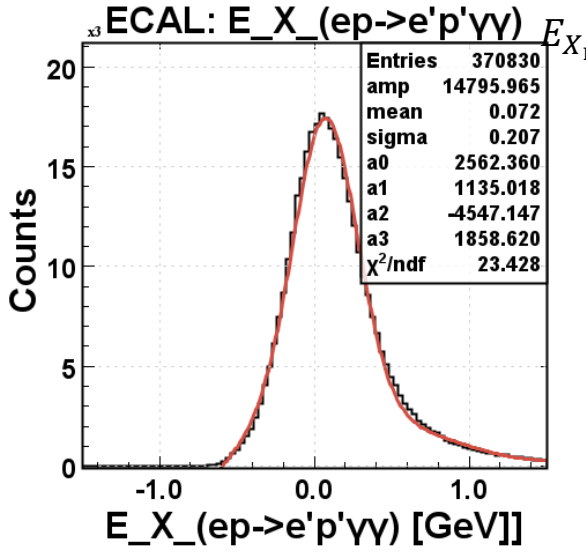

One set of cuts for $ep \to e'p'(\gamma\gamma)_{\pi^0}X$ requires both final-state photons to hit ECal.

7.5 GeV ECal-FTCal Cuts

$$\Delta\theta = \cos^{-1}\frac{\overrightarrow{\pi^0}\overrightarrow{\pi^0}_{\text{miss}}}{\left|\overrightarrow{\pi^0}\right|\left|\overrightarrow{\pi^0}_{\text{miss}}\right|}$$

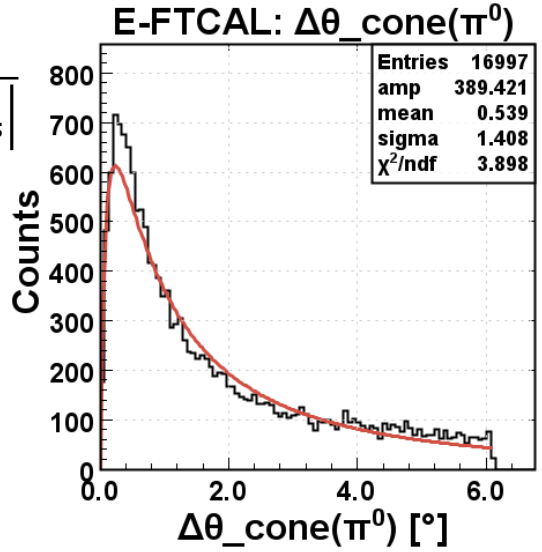

$$M_{p'_{\text{miss}}} = \sqrt{p'_{\text{miss}} \cdot p'_{\text{miss}}}$$

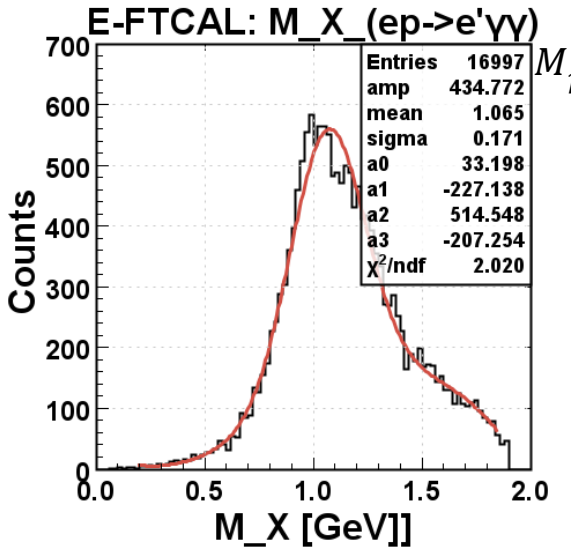

$X_{\text{miss}\perp}$

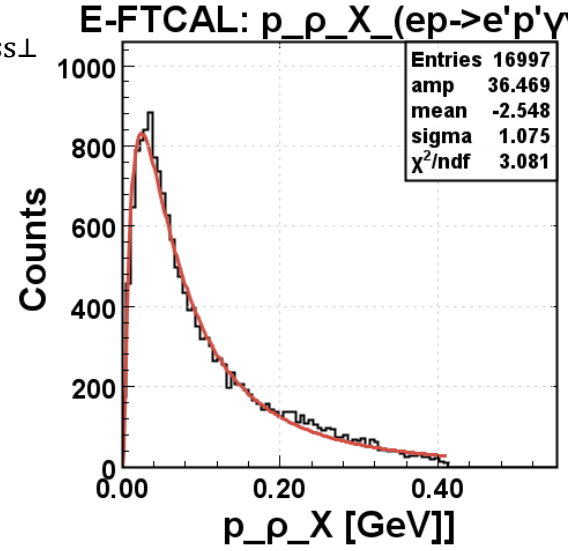

$E_{X_{\text{miss}}}$

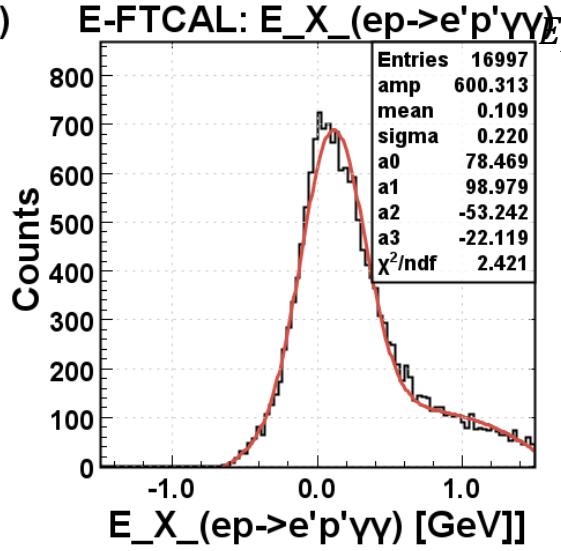

In $ep \to e'p'(\gamma\gamma)_{\pi^0}X$ reaction, one photon can hit ECal while the other lands on FTCal.

7.5 GeV FTCal-FTCal Cuts

$$\Delta\theta = \cos^{-1}\frac{\overrightarrow{\pi^0}\overrightarrow{\pi^0}_{\text{miss}}}{\left|\overrightarrow{\pi^0}\right|\left|\overrightarrow{\pi^0}_{\text{miss}}\right|}$$

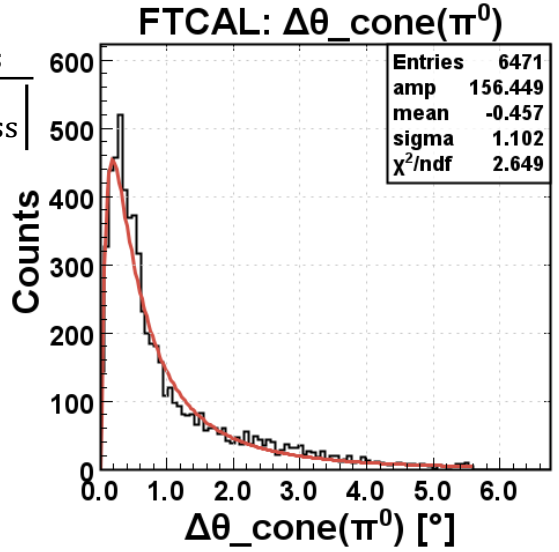

$$M_{p'_{\text{miss}}} = \sqrt{p'_{\text{miss}} \cdot p'_{\text{miss}}}$$

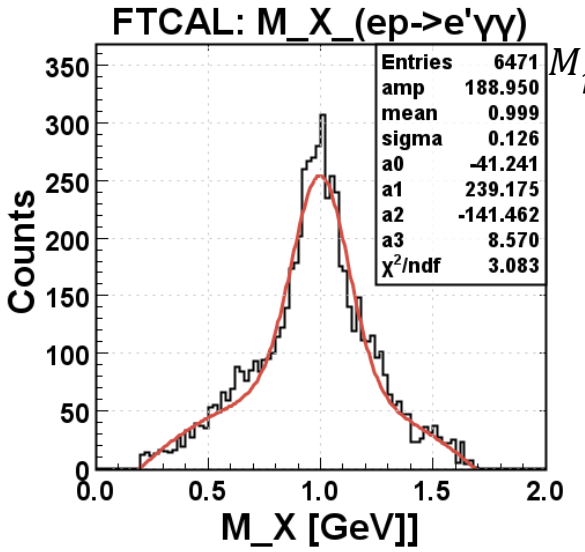

$X_{\text{miss}\perp}$

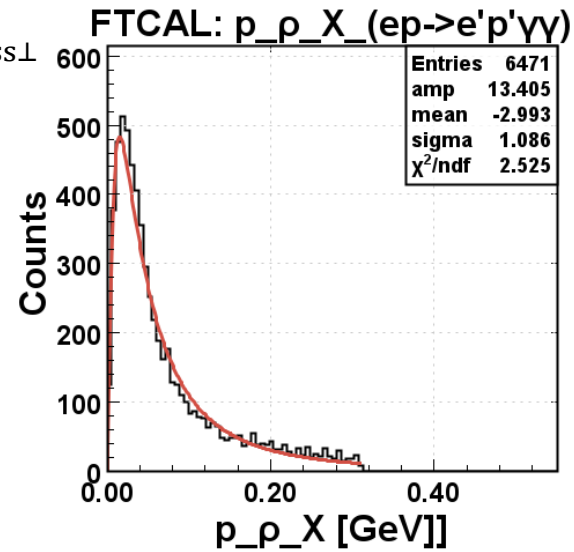

$E_{X_{\text{miss}}}$

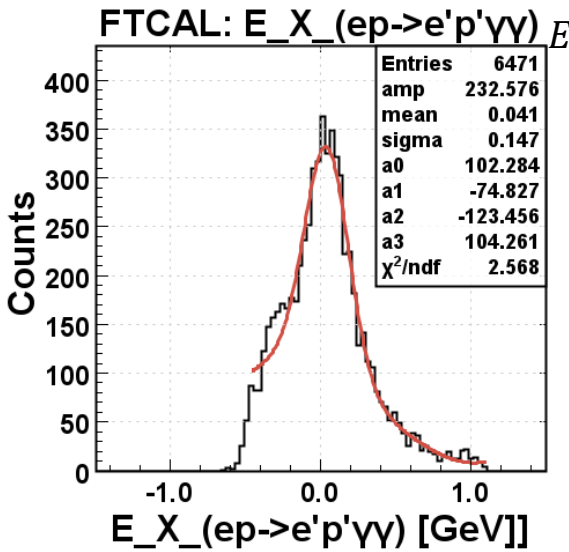

The third possible set of cuts for $ep \to e'p'(\gamma\gamma)_{\pi^0}X$ requires both final-state photons to hit FTCal.

π^0 Mass Cuts

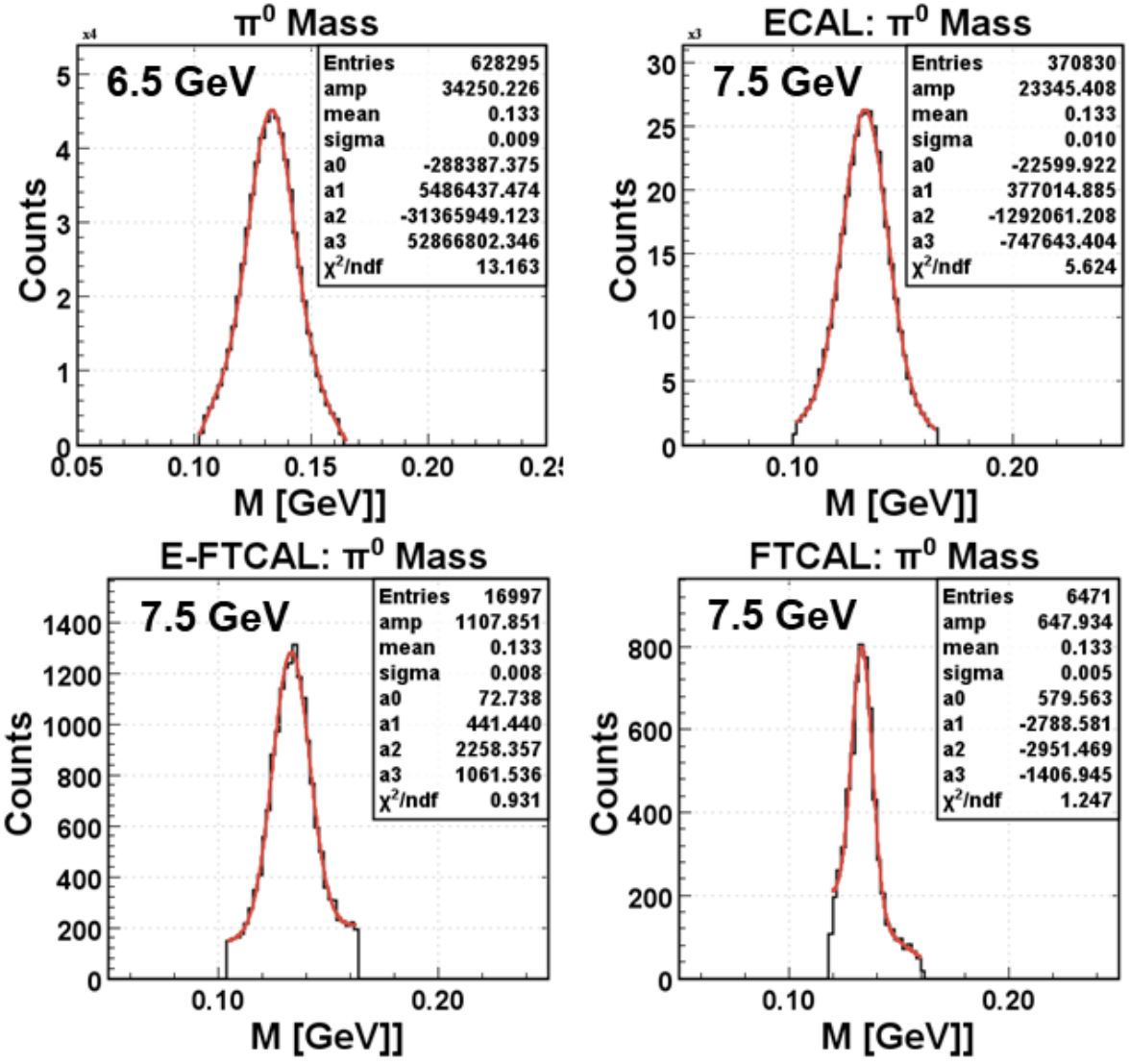

π^0 mass distributions rely mainly on the calorimeter resolutions.

Integrated DVπ^0P BSA

$A=\alpha \sin\phi$

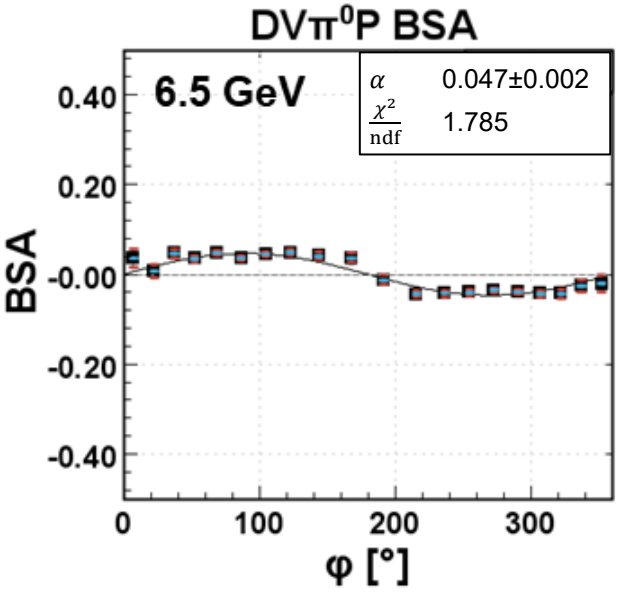

$A=\alpha \sin\phi$

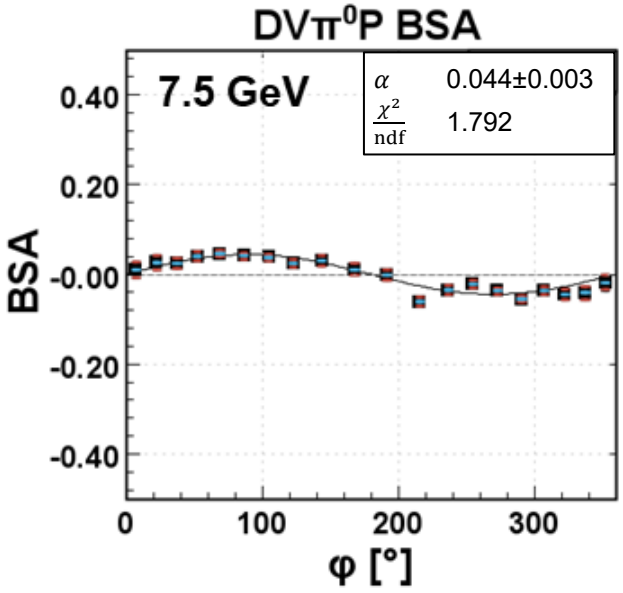

In the leading order DVπ^0P BSA only includes the $\sin\phi$ term.

6.5 GeV DVπ^0P BSA α

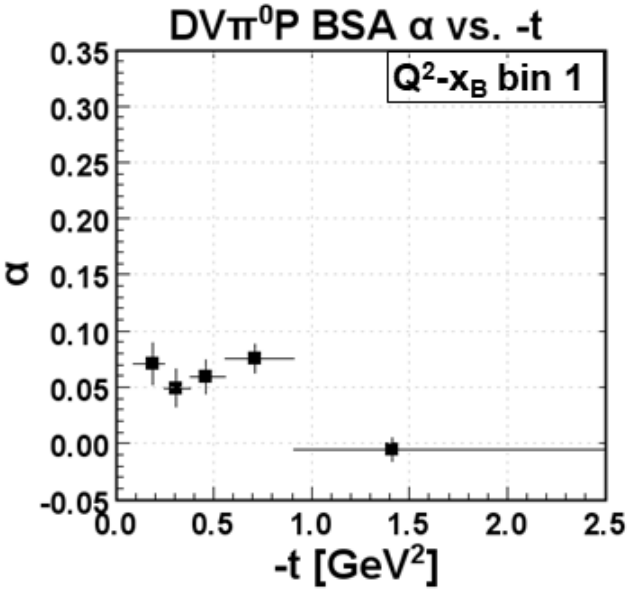

x_B < 0.17

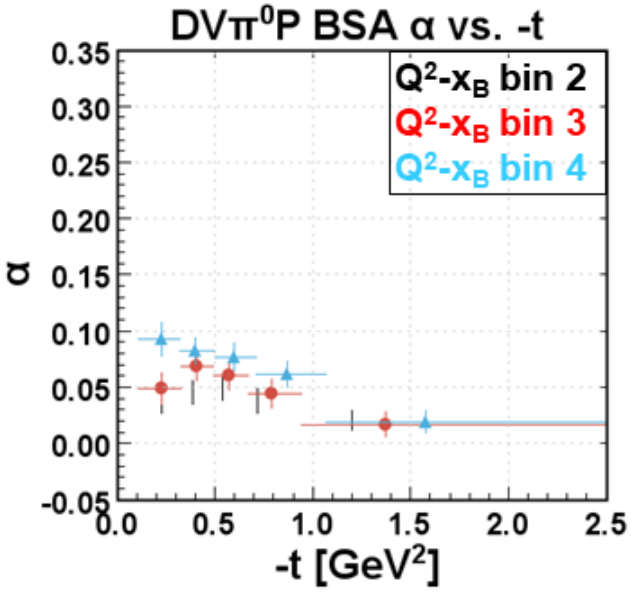

0.17 ≤ x_B < 0.27 :
Q^2 < 1.2 GeV²
1.2 GeV² ≤ Q^2 < 1.4 GeV²
1.4 GeV² ≤ Q^2

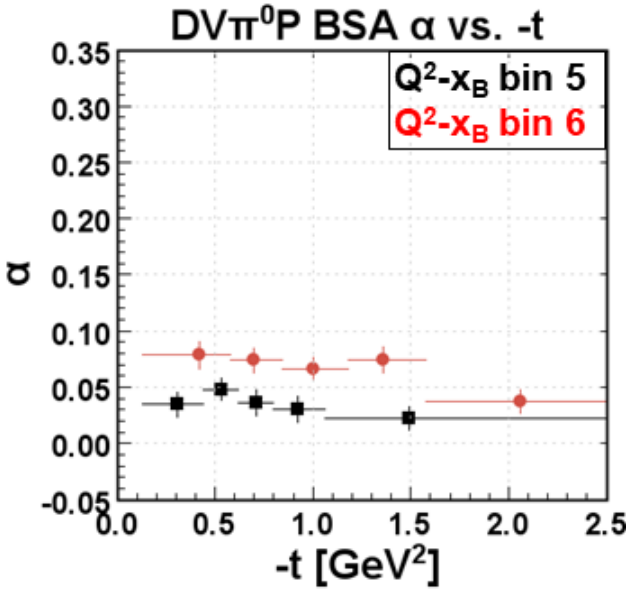

0.27 ≤ x_B :
Q^2 < 2.0 GeV²
2.0 GeV² ≤ Q^2

The same $(Q^2, x_B, -t)$ bins were adopted for DVπ^0P BSA analysis section.

7.5 GeV DVπ^0P BSA α

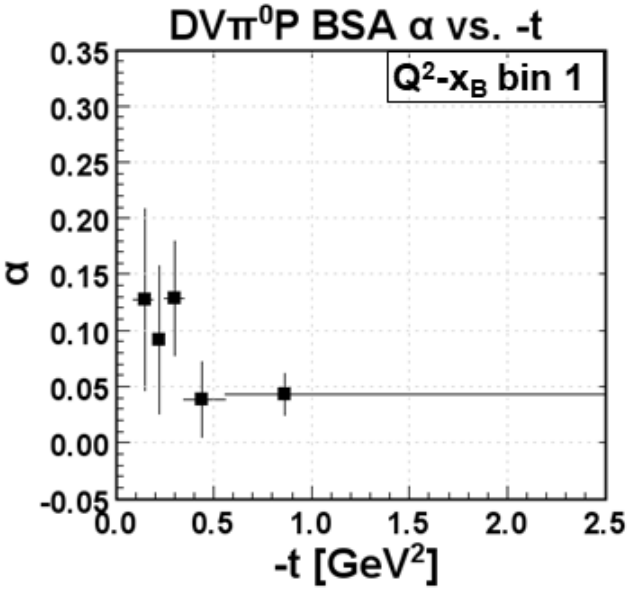

x_B < 0.13

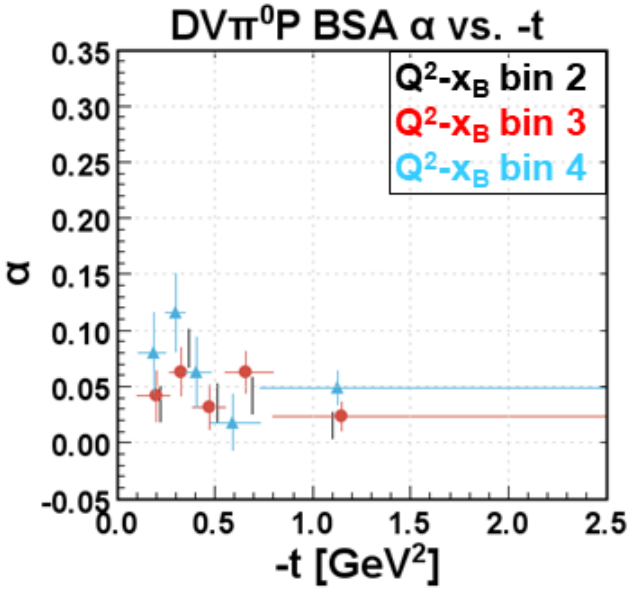

0.13 ≤ x_B < 0.22 :
Q^2 < 1.2 GeV²
1.2 GeV² ≤ Q^2 < 1.5 GeV²
1.5 GeV² ≤ Q^2

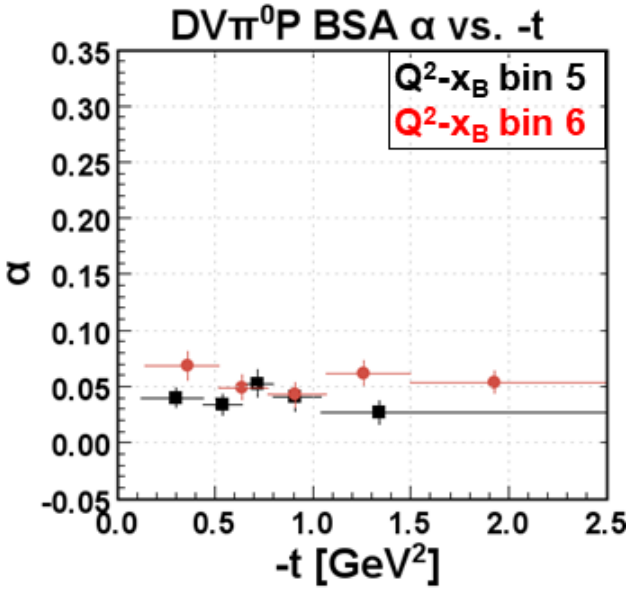

0.22 ≤ x_B :
Q^2 < 1.8 GeV²
1.8 GeV² ≤ Q^2

Since the binning was optimized for DVCS, $(Q^2, x_B, -t)$ bins of disproportionately high uncertainties can be observed.

DVπ^0P GEMC Simulations

Detector:
rgk_fall2018_FTOff
Magnetic field:
tor+1.00_sol-100
Background:
60nA_6535MeV

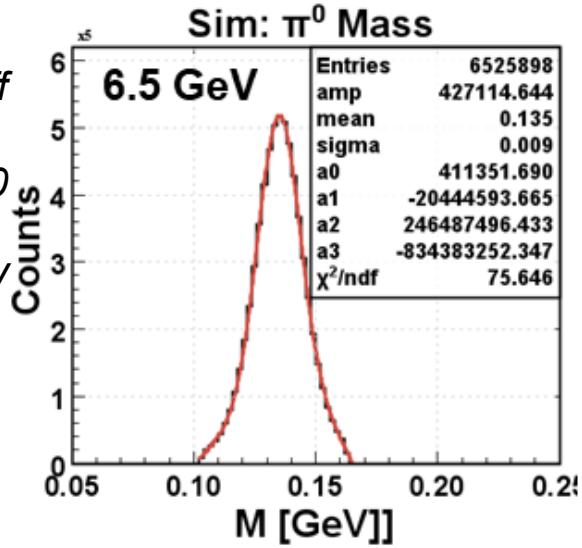

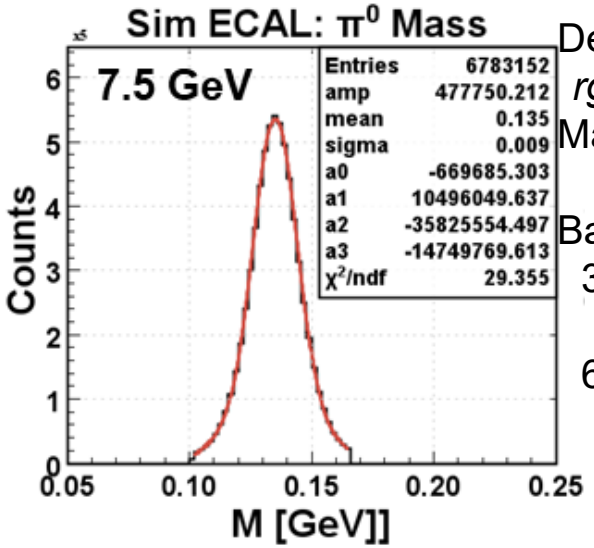

Detector:
rgk_fall2018_FTOn
Magnetic field:
tor+1.00_sol-100
Background:
36.4% at
35nA_7546MeV
63.6% at
45nA_7546MeV

Detector:
rgk_fall2018_FTOn
Magnetic field:
tor+1.00_sol-100
Background:
36.4% at
35nA_7546MeV
63.6% at
45nA_7546MeV

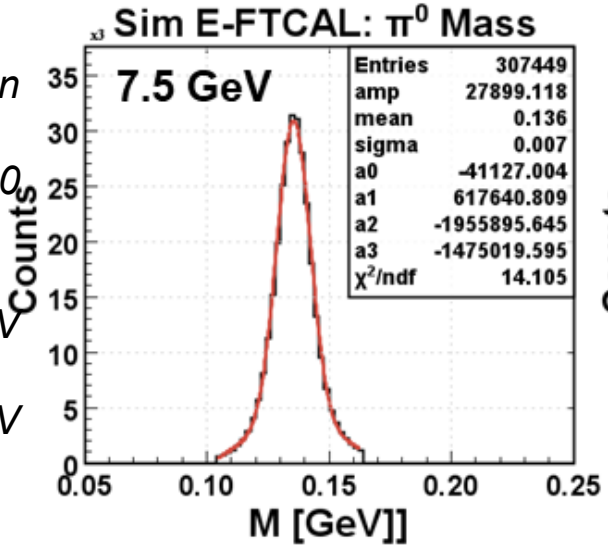

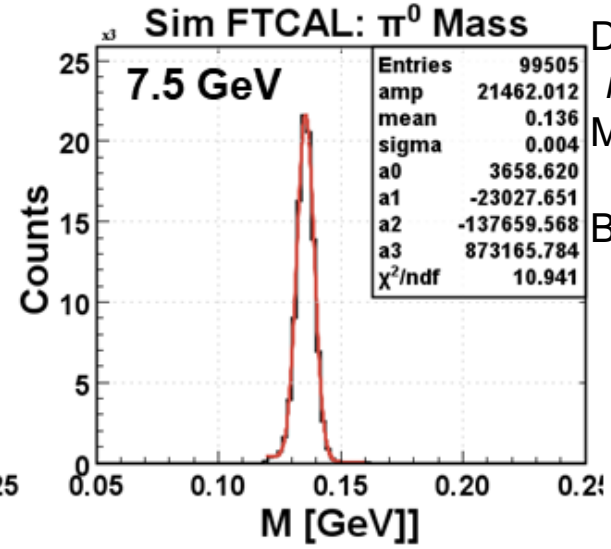

π^0 invariant mass distributions from the simulations are in good agreement with the ones from the data.

Integrated Fractional Contamination

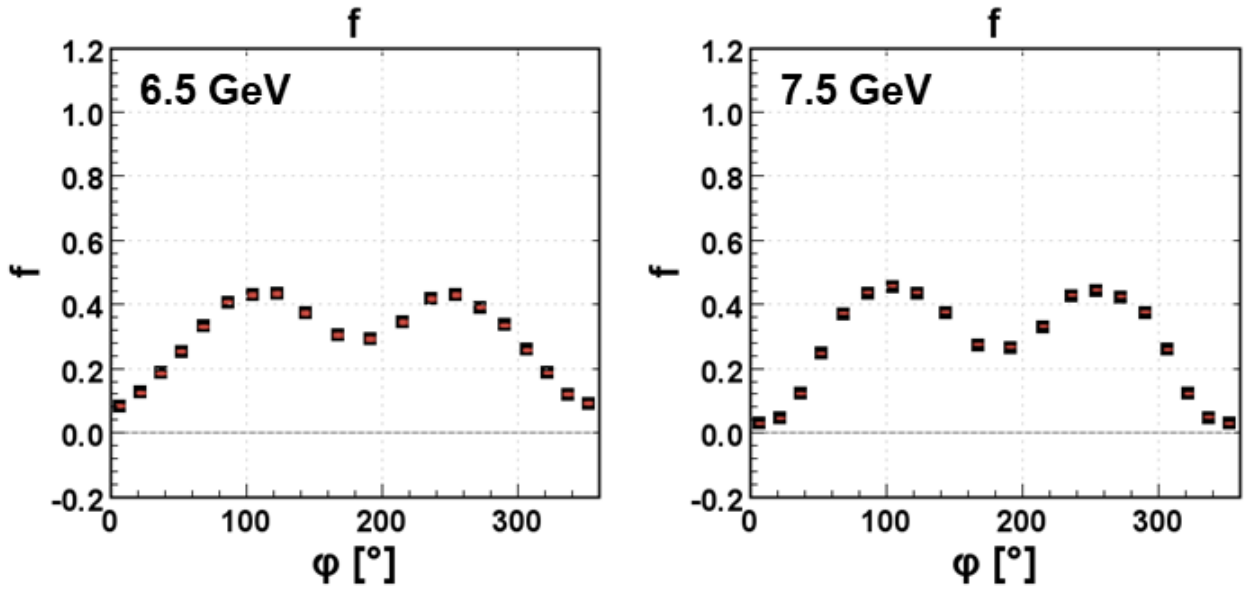

The fractional contamination f quantifies the contribution of DVπ^0P BSA to $ep\gamma$ BSA. f can also be estimated using fast MC.

π^0 Events from Fast MC

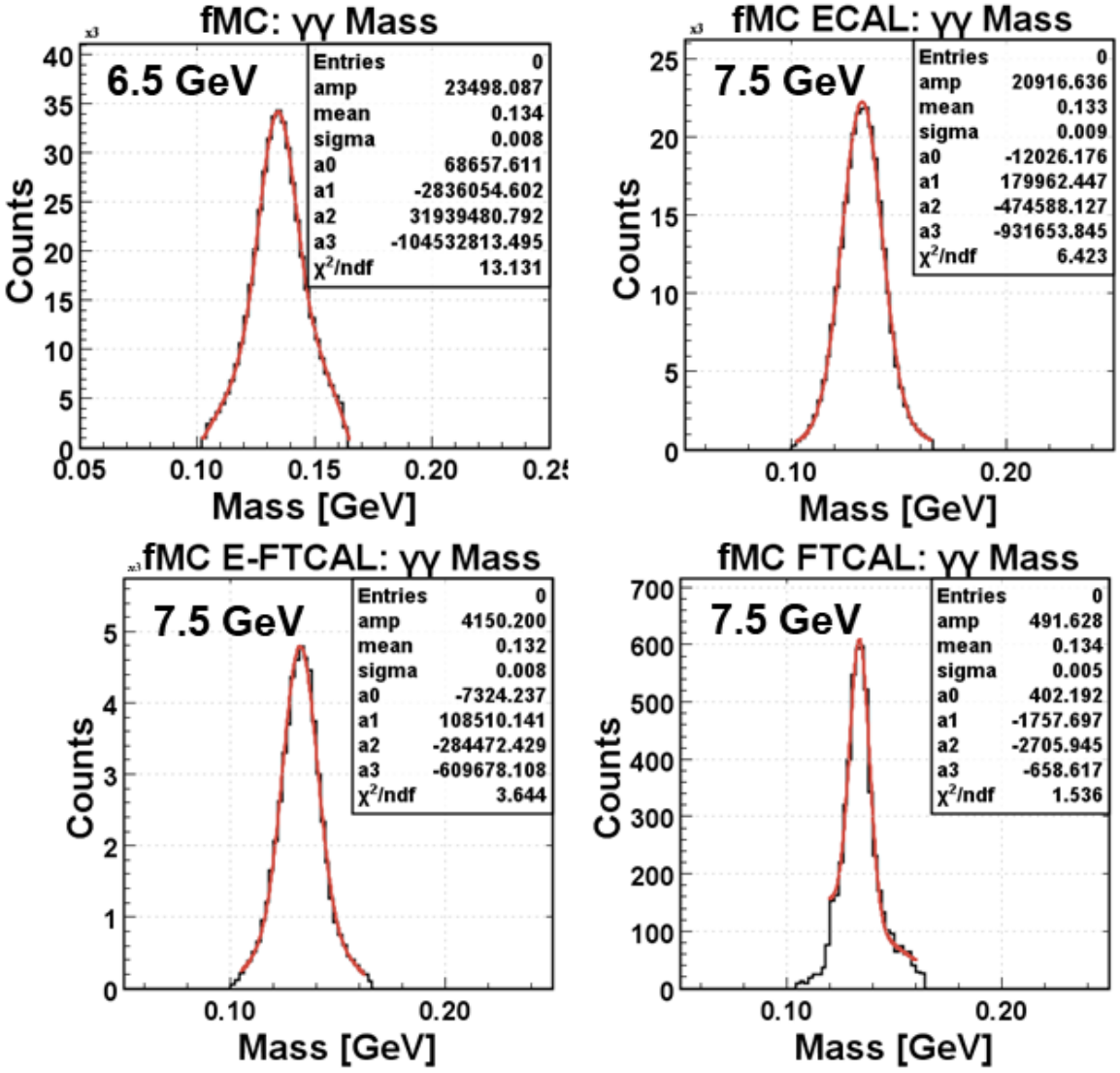

Photon resolution smearing produced consistent fMC π^0 invariant mass distributions.

Integrated f from fMC

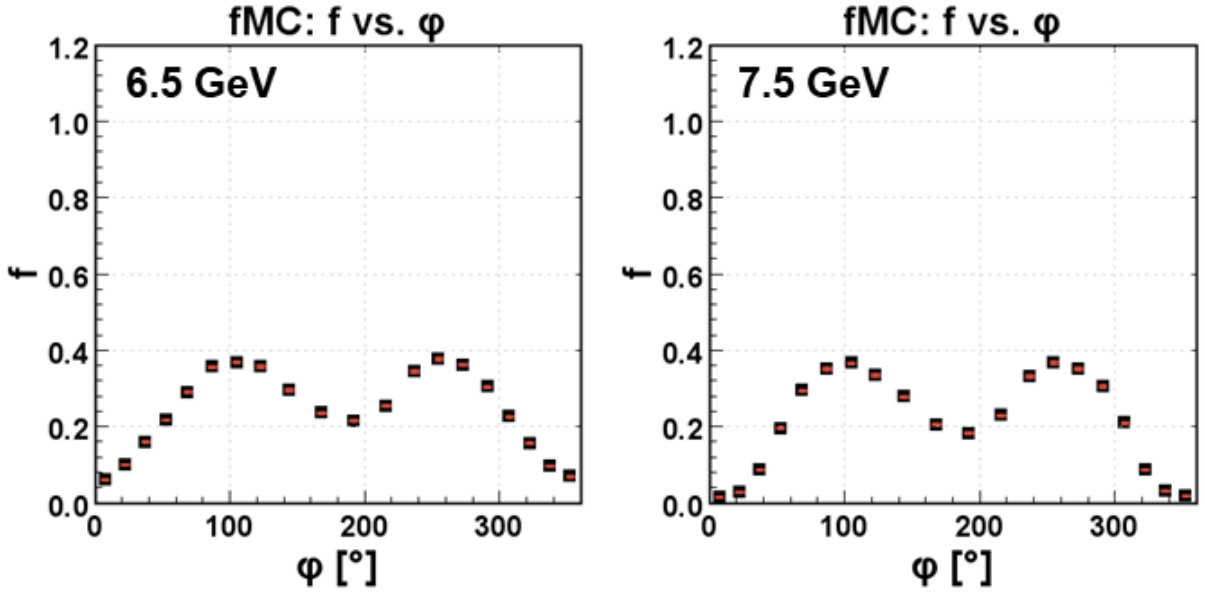

f estimates from fast MC were in good level of agreement with the estimates from GEMC simulations.

Systematic Errors

Polarization Uncertainty

$$A = \frac{\alpha \sin\phi}{1 + \beta \cos\phi}$$

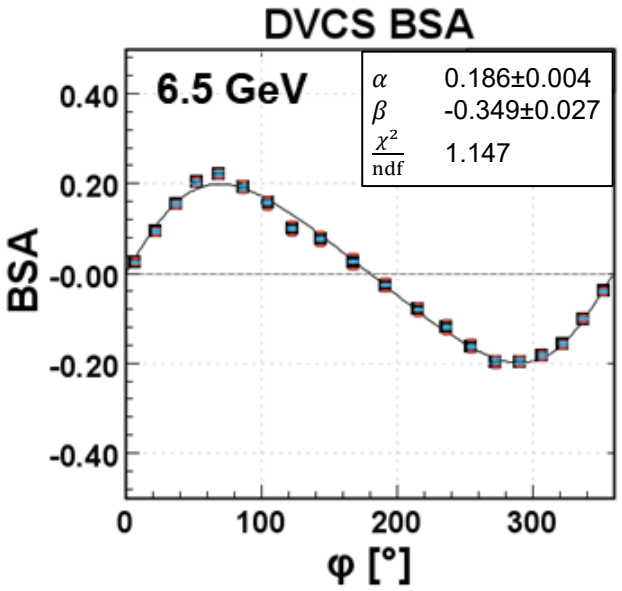

$$A = \frac{\alpha \sin\phi}{1 + \beta \cos\phi}$$

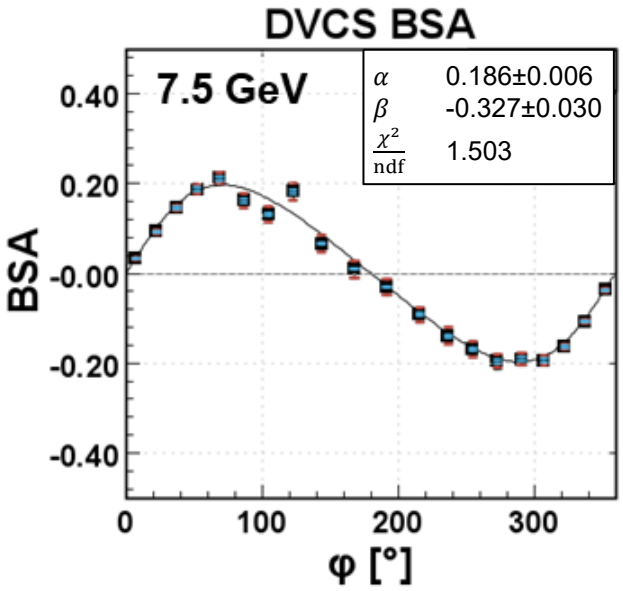

E_{beam} [GeV]	Fit	Parameters	σ_{syst}
6.535	$\frac{\alpha \sin\phi}{1 + \beta \cos\phi}$	$\alpha = 0.186 \pm 0.00412$	0.000806
		$\beta = -0.349 \pm 0.0269$	0.00156
7.546	$\frac{\alpha \sin\phi}{1 + \beta \cos\phi}$	$\alpha = 0.186 \pm 0.00550$	0.000278
		$\beta = -0.327 \pm 0.0301$	0.000182

Systematic variations were calculated in reference to the values obtained without any systematic uncertainty.

π^0 Contamination Uncertainty

$$A = \frac{\alpha \sin\phi}{1 + \beta \cos\phi}$$

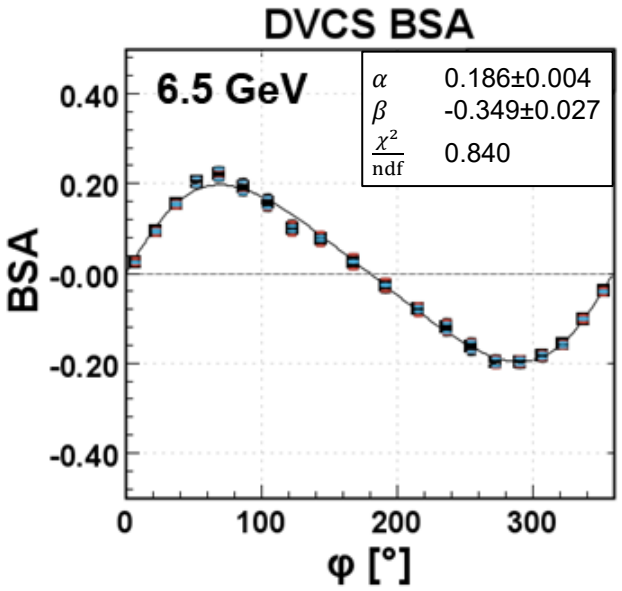

$$A = \frac{\alpha \sin\phi}{1 + \beta \cos\phi}$$

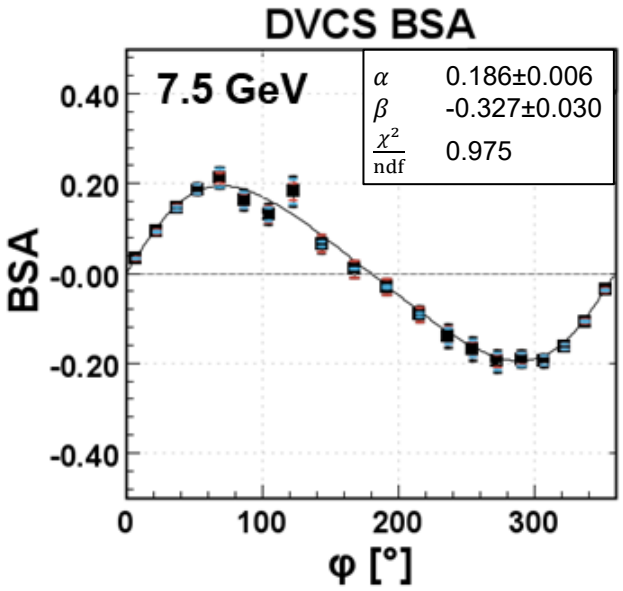

E_{beam} [GeV]	Fit	Parameters	σ_{syst}
6.535	$\frac{\alpha \sin\phi}{1 + \beta \cos\phi}$	$\alpha = 0.185 \pm 0.00503$	0.00235
		$\beta = -0.348 \pm 0.0306$	0.000135
7.546	$\frac{\alpha \sin\phi}{1 + \beta \cos\phi}$	$\alpha = 0.184 \pm 0.00748$	0.00284
		$\beta = -0.336 \pm 0.0369$	0.00939

Uncertainty in f (Δf) collectively includes the convoluted effects of fiducial and exclusivity cut systematics.

6.5 GeV: Δf Effects in α

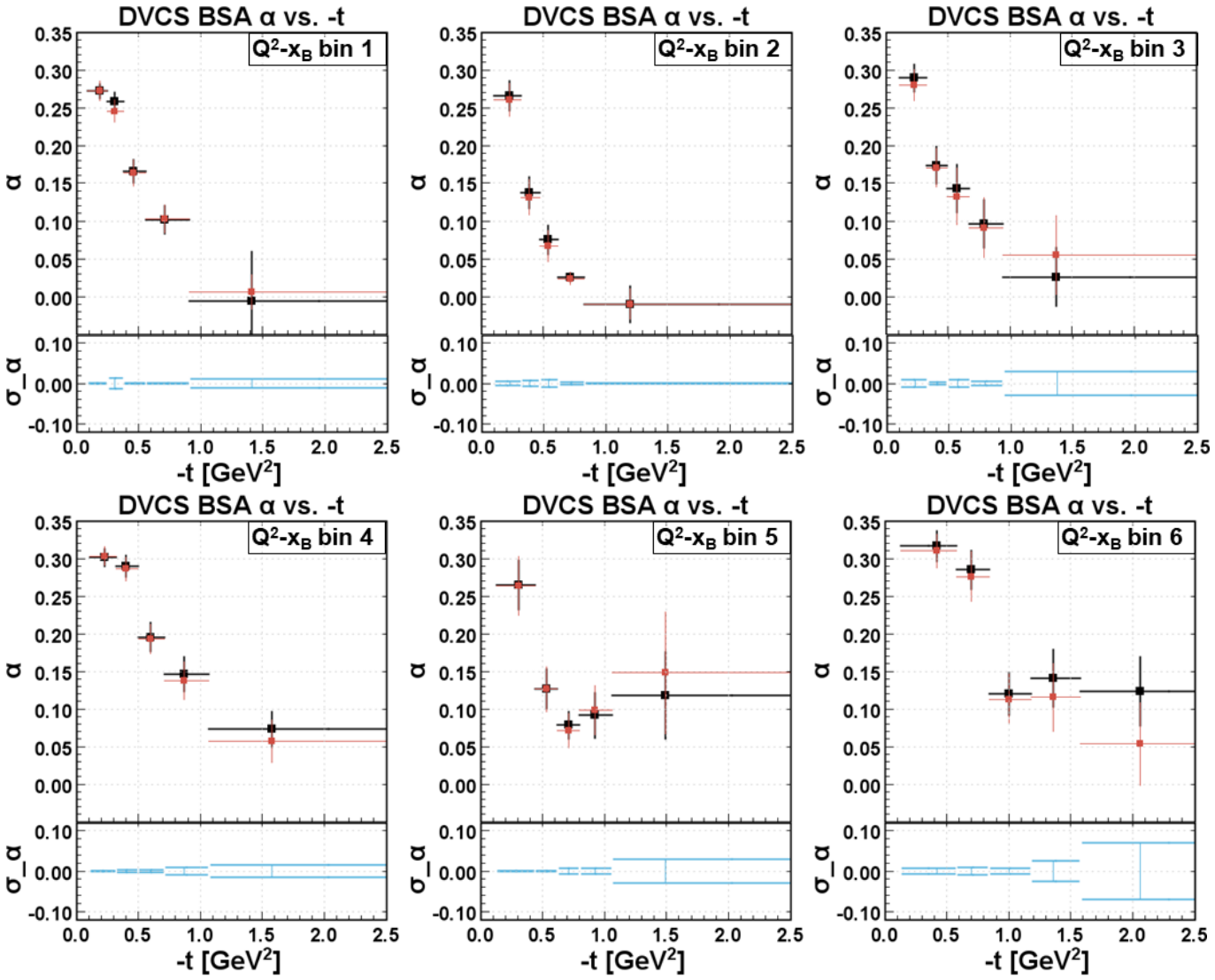

Values of α were extracted with (red) and without (black) the inclusion of Δf.

7.5 GeV: Δf Effects in α

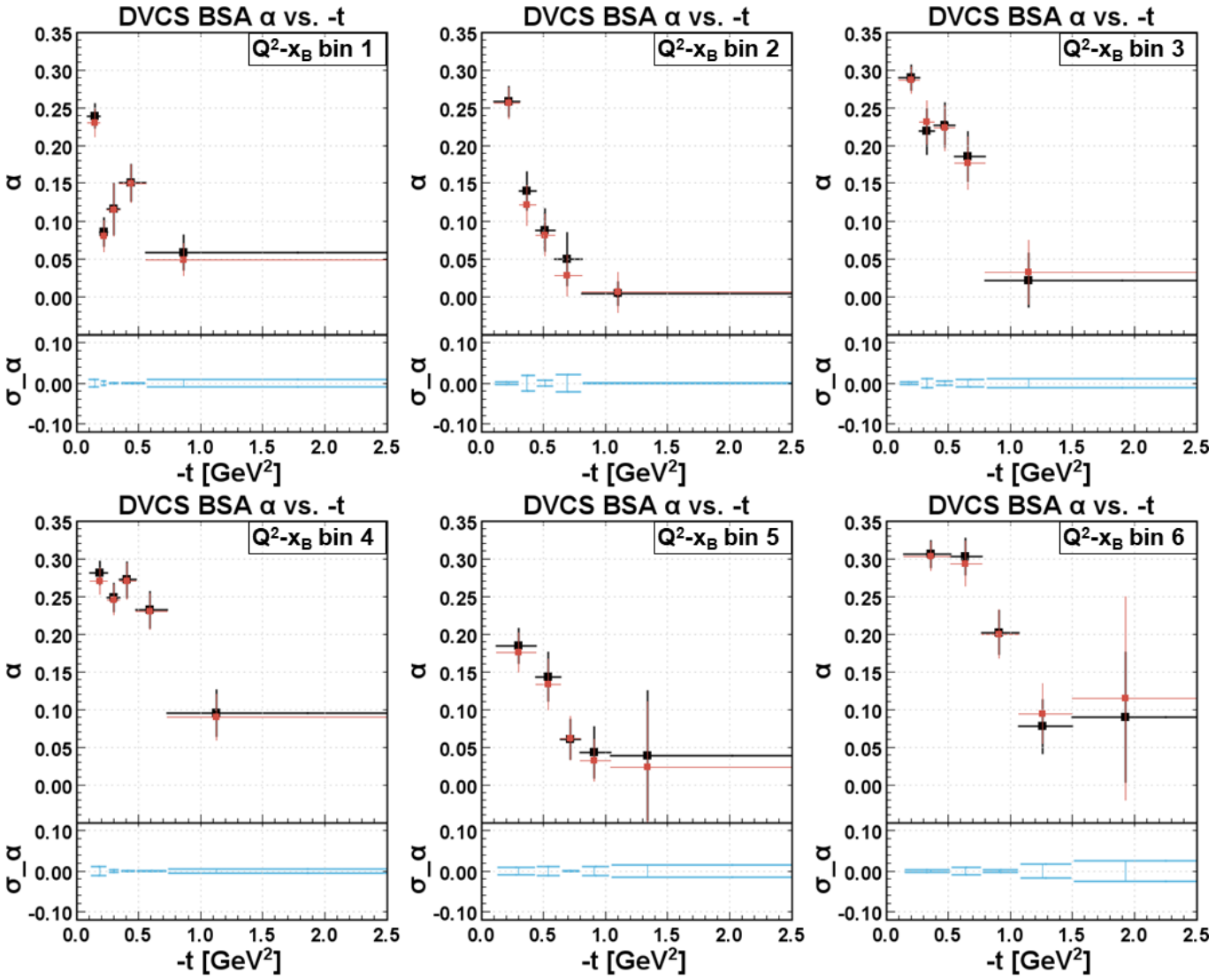

In general, the systematic variation in α due to Δf is smaller than the error due to statistical uncertainties.

6.5 GeV: Δf Effects in β

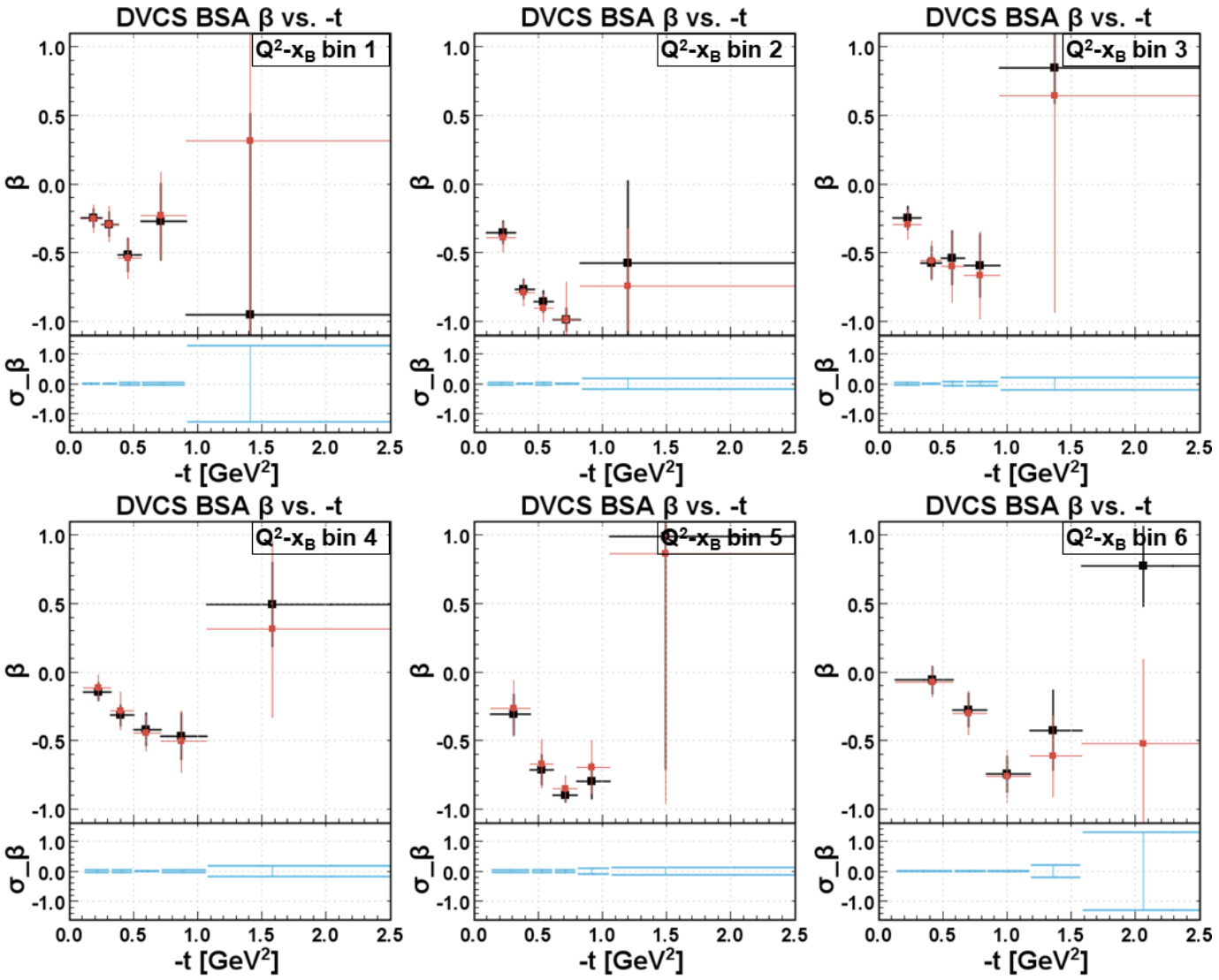

Systematic variation in β has tendency to increase in high $-t$ regions.

7.5 GeV: Δf Effects in β

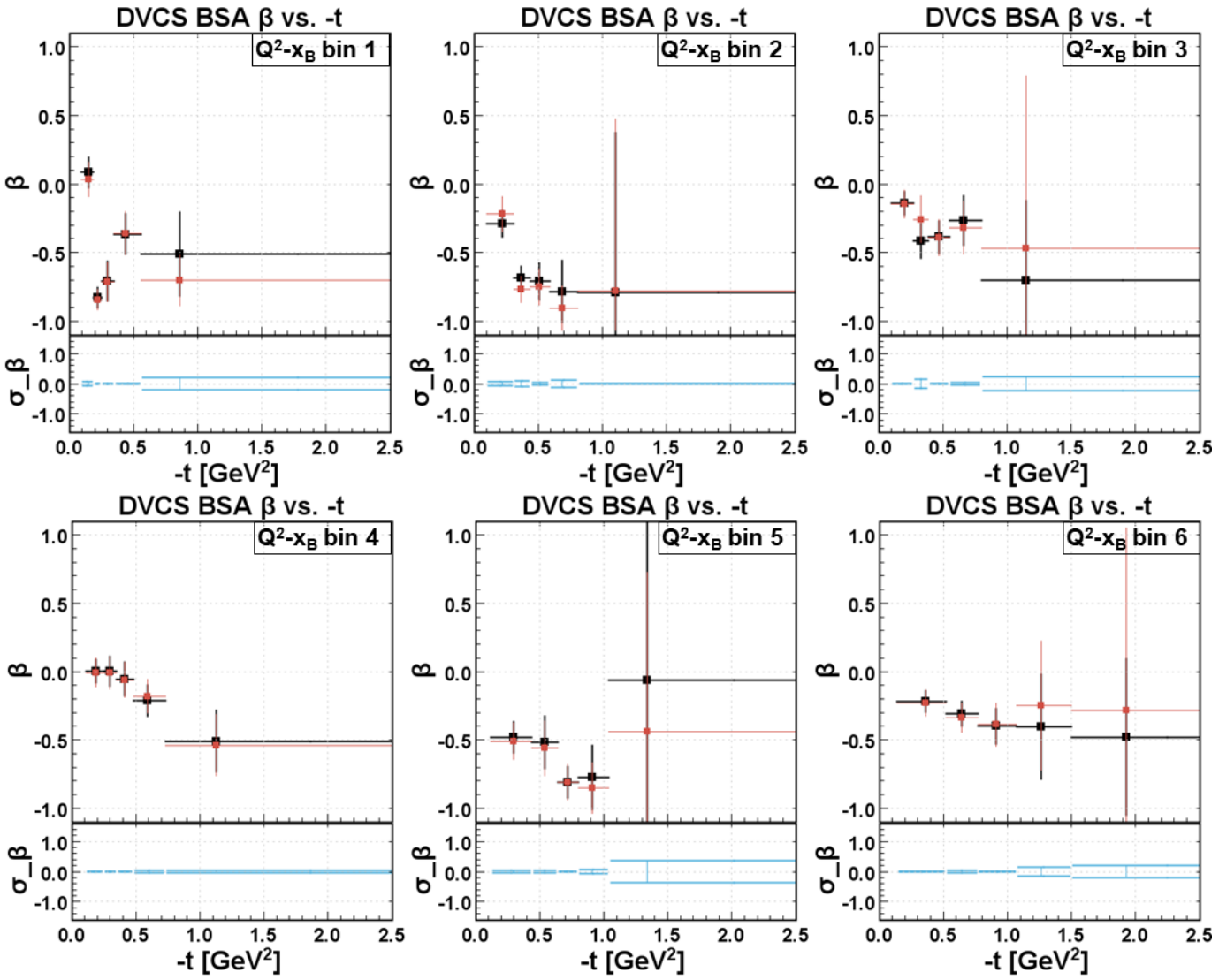

The systematic variation in β due to Δf is generally less than the error due to statistical uncertainties.

Fully Corrected BSA

Corrected DVCS BSA (Integrated)

$$A = \frac{\alpha \sin\phi}{1 + \beta \cos\phi}$$

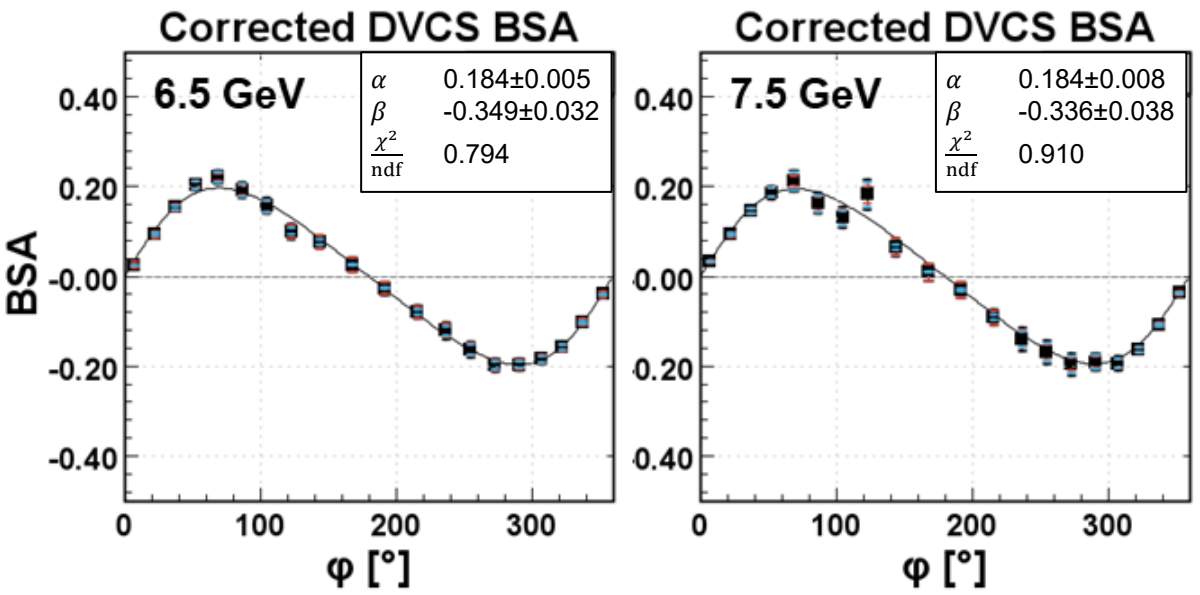

$$A = \frac{\alpha \sin\phi}{1 + \beta \cos\phi}$$

Fully corrected DVCS BSA was measured after π^0 contamination subtraction and includes all statistical and systematic uncertainties.

6.5 GeV Corrected DVCS BSA α

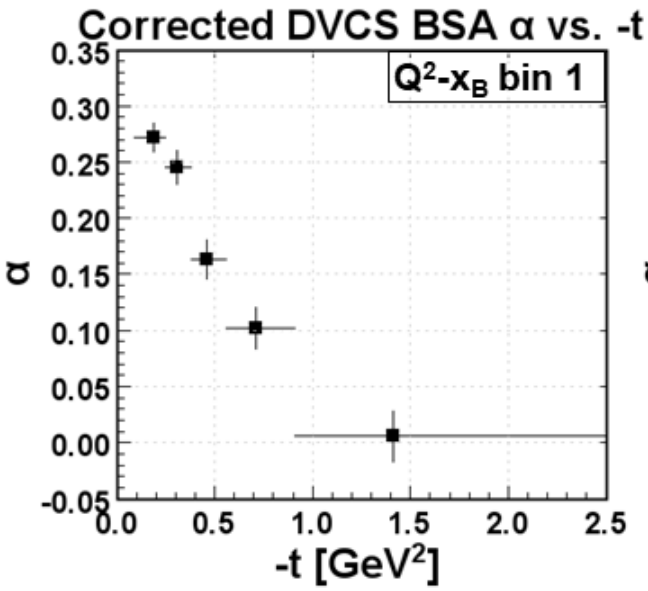

x_B < 0.17

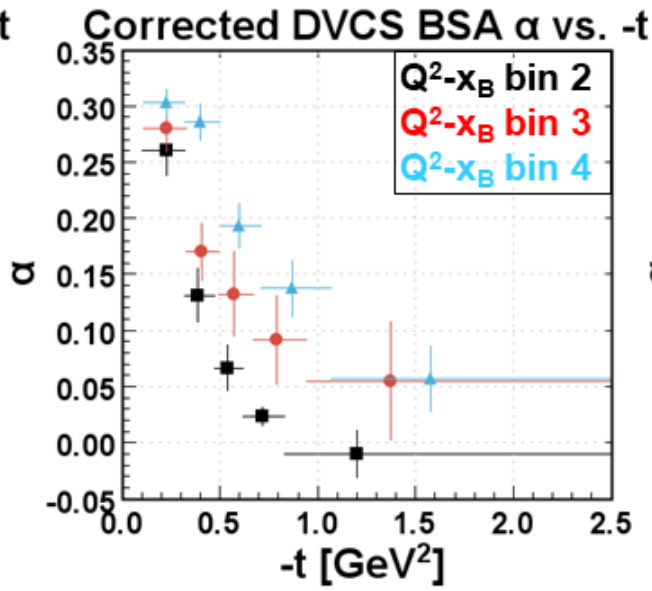

0.17 ≤ x_B < 0.27 :
Q^2 < 1.2 GeV²
1.2 GeV² ≤ Q^2 < 1.4 GeV²
1.4 GeV² ≤ Q^2

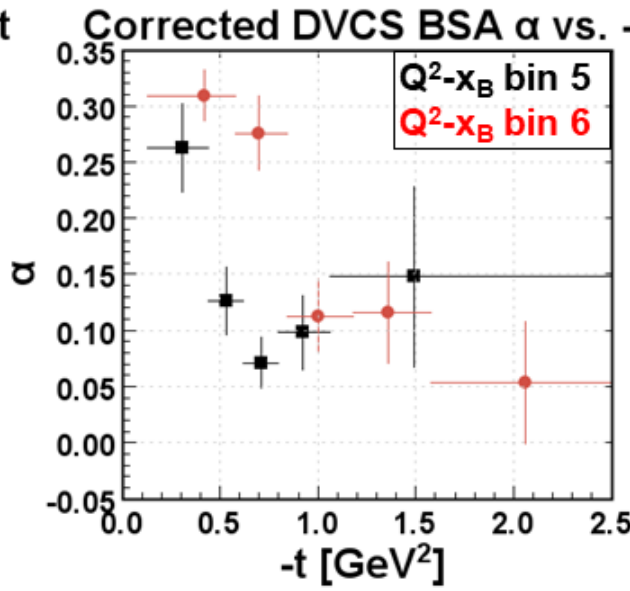

0.27 ≤ x_B :
Q^2 < 2.0 GeV²
2.0 GeV² ≤ Q^2

Comparison with raw BSA measurements shows higher sensitivity of the uncertainties to π^0 contamination subtraction in high Q^2, high x_B, and high $-t$ regions.

7.5 GeV Corrected DVCS BSA α

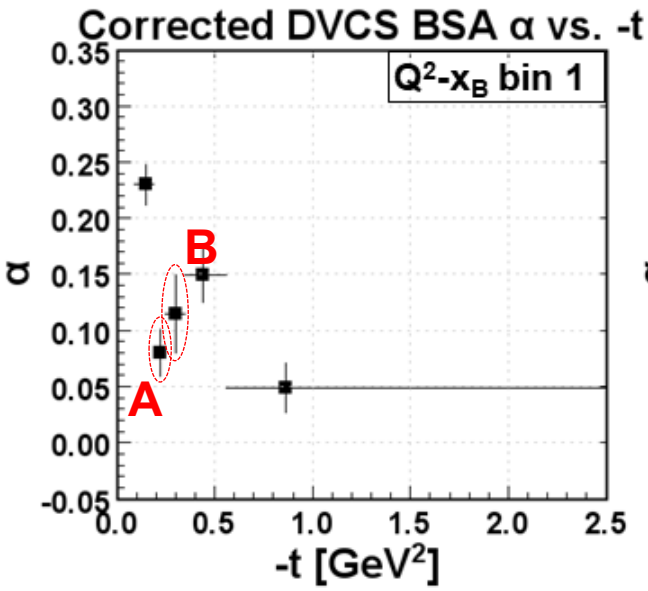

x_B < 0.13

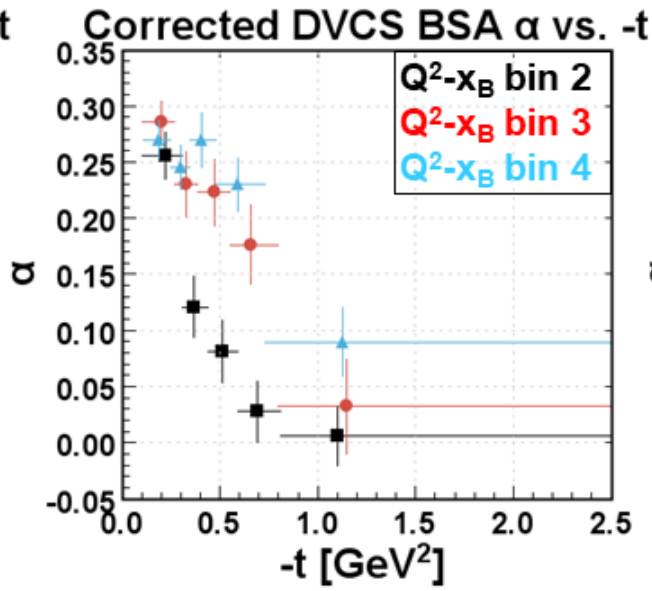

0.13 ≤ x_B < 0.22 :
Q^2 < 1.2 GeV²
1.2 GeV² ≤ Q^2 < 1.5 GeV²
1.5 GeV² ≤ Q^2

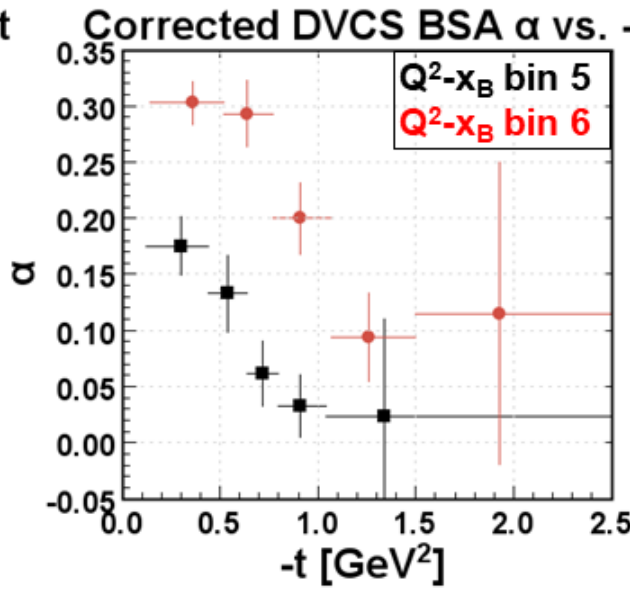

0.22 ≤ x_B :
Q^2 < 1.8 GeV²
1.8 GeV² ≤ Q^2

The same “out-of-trend” measurements (**A** and **B**) can be observed after π^0 contamination subtraction.

7.5 GeV Low Statistics Bins

$$A = \frac{\alpha \sin\phi}{1 + \beta \cos\phi}$$

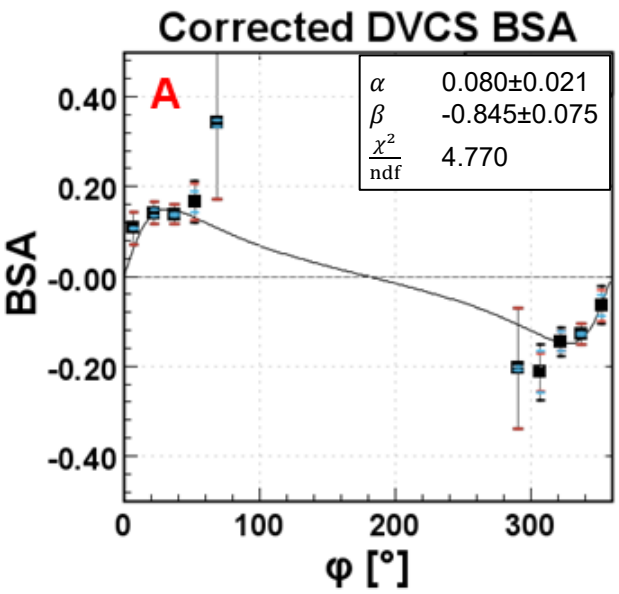

$$A = \frac{\alpha \sin\phi}{1 + \beta \cos\phi}$$

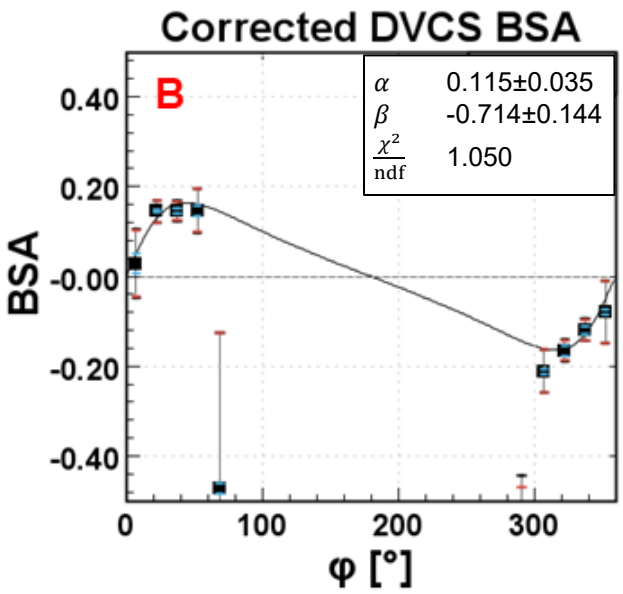

Closer look to the "out-of-trend" α measurements shows that their corresponding $(Q^2, x_B, -t)$ bins lacked statistics in ϕ.

6.5 GeV Corrected DVCS BSA β

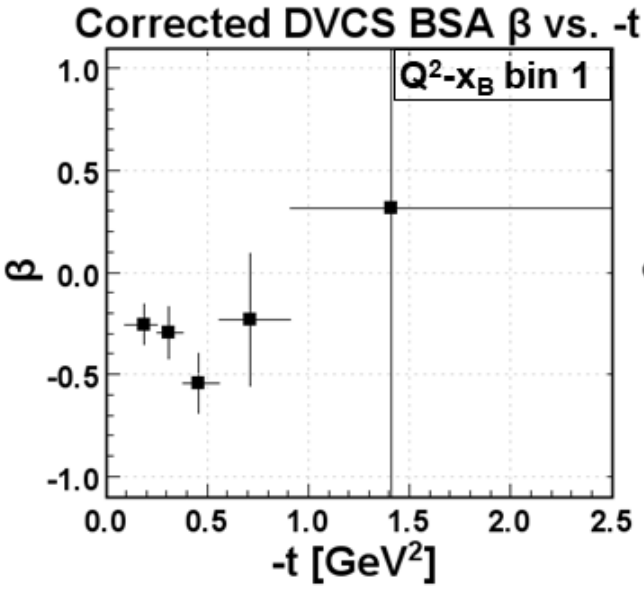

x_B < 0.17

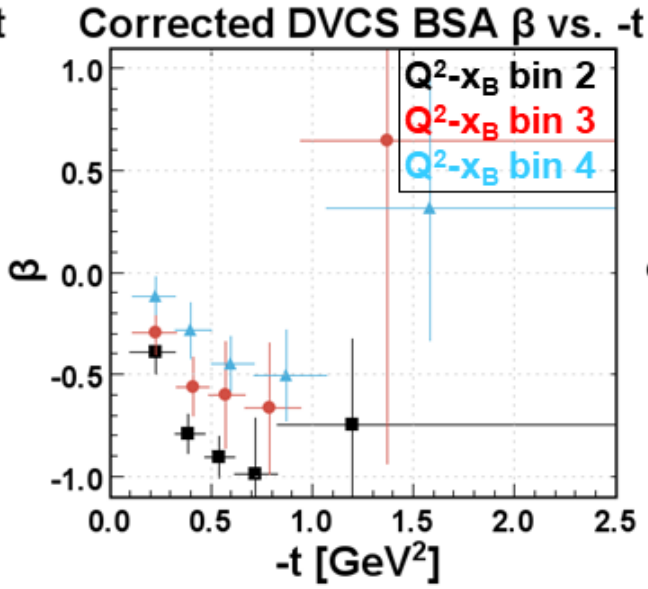

0.17 ≤ x_B < 0.27 :
Q^2 < 1.2 GeV²
1.2 GeV² ≤ Q^2 < 1.4 GeV²
1.4 GeV² ≤ Q^2

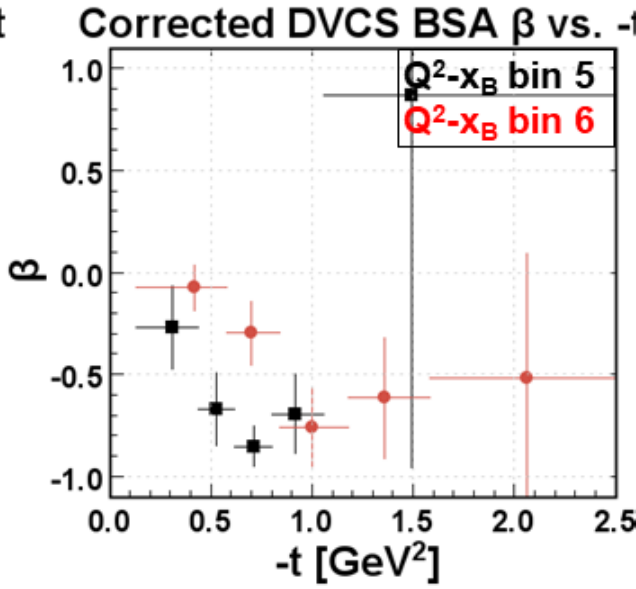

0.27 ≤ x_B :
Q^2 < 2.0 GeV²
2.0 GeV² ≤ Q^2

Like measurements in α, the errors in β increases in high Q^2, high x_B, and high $-t$ regions.

7.5 GeV Corrected DVCS BSA β

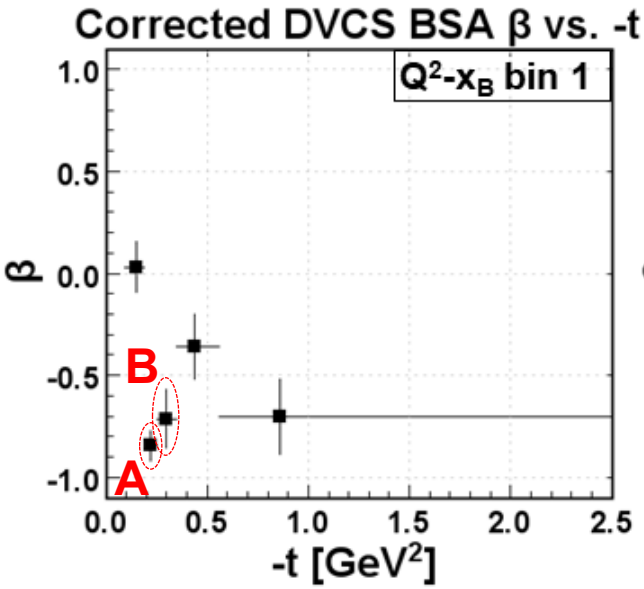

x_B < 0.13

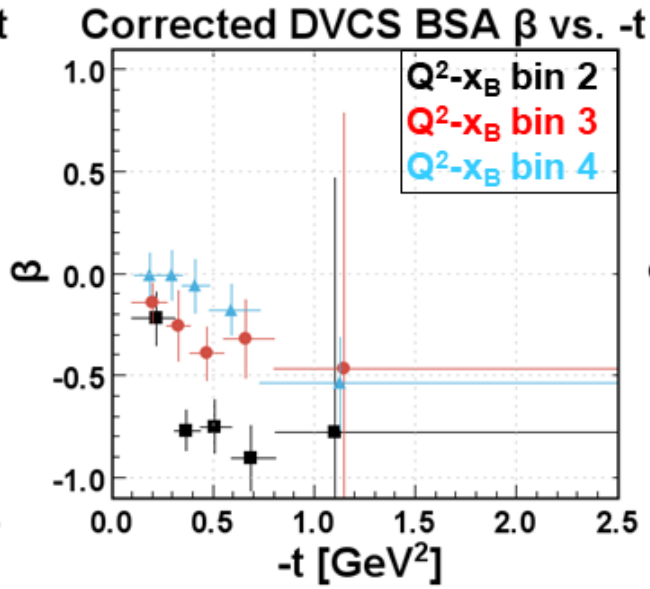

0.13 ≤ x_B < 0.22 :
Q^2 < 1.2 GeV²
1.2 GeV² ≤ Q^2 < 1.5 GeV²
1.5 GeV² ≤ Q^2

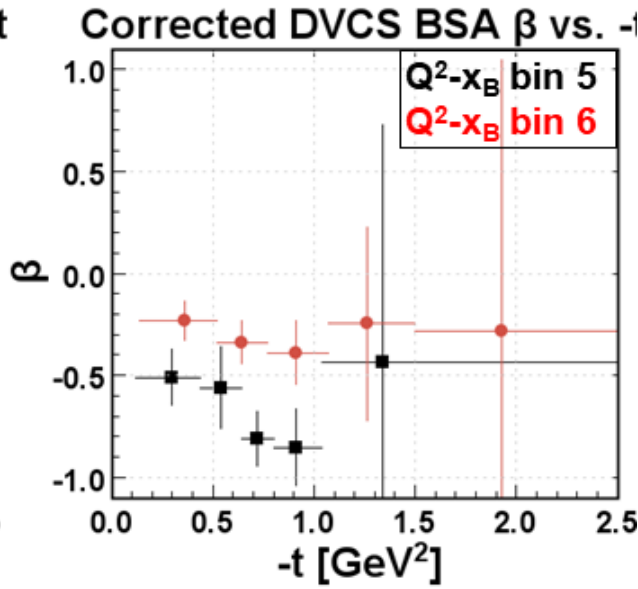

0.22 ≤ x_B :
Q^2 < 1.8 GeV²
1.8 GeV² ≤ Q^2

Although the errors of "out-of-trend" measurements (**A** and **B**) are small in β, individual inspections of their bins conclusively suggest the unreliable results from these bins.

Summary

In this analysis:

- DVCS BSA was measured at 6.5 GeV and 7.5 GeV beam energies.
- $(Q^2, x_b, -t)$ -dependence of BSA measurements was mapped.
- π^0 contaminants were estimated, and their asymmetry contributions were excluded.
- Systematic uncertainties were contained within the range of statistical errors.
- The H-GPD-sensitive observable α was extracted with values comparable to earlier measurements.

Following this analysis:

- The corresponding DVCS cross-section will be measured from the same data set.
- The BSA measurements acquired will be used as constraints in H GPD extraction.
- Investigation of the nature and behavior of the detected $ep\gamma$ events at high $-t$ can be conducted.

Thank You!!!